TG – TGO 2022

Influence of Electrode Location, BMI, and Sex on Skin Sympathetic Nerve Activity Measurements in Healthy Subjects

Niels Bergwerff (S2310465)
Nathan Van Dieren (S2306158)
Laura Dolmans (S2274299)
Thijs Voortman (S2253615)

Medical Supervisor MST: Drs. V.R. van der Pas
Technological Supervisor UT: Dr. Y. Wang
Technological Supervisor MST: Dr. F.R. Halfwerk & J.W. Tertoolen
Process Supervisor: Dr. M. Groenier
Tutor: J.L. van Steenis

27-6-2022

UNIVERSITY OF TWENTE.

Abstract

Introduction: In patients with recurring arrhythmias after myocardial infarction, suppression of the sympathetic innervation of the heart can be a solution. A stellate ganglion block can provide this suppression, but first it needs to be determined if the arrhythmias are caused by overstimulation of the sympathetic nervous system. This could be proven by a temporary block of the stellate ganglion. To make sure that the temporary block works and suppresses the sympathetic activity, the nerve activity is measured. This can be done with skin sympathetic nerve activity (SKNA) measurements. This study aimed to determine the influence of sex, Body Mass Index (BMI), and electrode location on these measurements.
Materials and methods*:* In this study, the SKNA signals of six different lead positions were measured on 47 healthy participants. Stationary wavelet denoising was used to denoise the filtered SKNA signal. The different lead positions were compared on signal-to-noise ratios (SNR). The lead with the highest SNR was selected to test the statistical significance of the differences between BMI groups and sex.
Results: It was found that the thorax leads had a better SNR than the arm leads. Thorax lead II and III were the best lead positions for measuring SKNA in this research population, based on the SNR. BMI and sex were found to have a statistically significant difference between groups, although interactions could not be tested.
Conclusion: Future research on SKNA measurements can best be done with electrode positions on the chest. There is an indication that BMI and sex have some influence on the SKNA signal, but because of the nonrepresentative study population, definitive conclusions cannot be made. These influences need to be investigated further with a larger and more representative study population.

Introduction

In 2020, cardiovascular disease was the second cause of death in the Netherlands. In 2020 alone, 36 thousand people died due to cardiovascular disease and 13% of these deaths could be attributed to myocardial infarction (MI) [1]. However, even if a patient survives an MI, a patient can suffer from long-term consequences. One of these long-term consequences is the development of ventricular arrhythmias (VAs), caused by progressive remodelling of the myocardium [2]. The current treatment for these persistent VAs consists of medication (beta blockers), ablation, and/or an implantable cardioverter-defibrillator [3]. However, in some cases, patients experience recurring arrhythmias even after they have received these treatments, which can have a large impact on the patients' quality of life.

In recent years, studies have shown that in patients suffering from heart failure (HF) or MI, the autonomic innervation of the heart is often disturbed. This results in an increase in the sympathetic tone. This increase can be ascribed to several pathological mechanisms in the control and activation of the sympathetic nervous system [4]. The increase in sympathetic stimulation has several effects in patients with HF and MI. In combination with altered parasympathetic activity, this can increase the risk of atrial fibrillation. An increase in sympathetic tone has also been shown to precede instances of ventricular tachycardia [5].

The treatment of recurrent VAs sometimes fails because the arrhythmias are caused by increased sympathetic activity. However, recently, studies have shown that a block of the sympathetic innervation of the heart could be an effective way to treat these recurrent VAs. In this treatment, the stellate ganglion, which provides the sympathetic innervation of the ventricles, is blocked [6,7]. To test if a complete block could be beneficial for a given patient, a temporary block can be performed. In this procedure, an anesthetic is injected into the stellate ganglion to temporarily block the nerves that innervate the ventricles. If this blockade suppresses VAs, this is an indication that a permanent surgical block could be beneficial [6]. However, if a temporary block does not alleviate the arrhythmias, it is not possible to differentiate whether there is an incomplete block or that there is another cause for the VAs.

To ascertain that VAs are caused by an increased sympathetic tone, the sympathetic nerve activity must be measured. Common ways to measure the autonomic activity are measuring the heart rate variability or measuring the nerve activity using microneurography. However, these methods have important limitations. Microneurography of the stellate ganglion is invasive, and heart rate variability is not always a representative estimate of sympathetic activity if the patient already takes drugs or treatment that influences measured activity [8]. Because of this, there is need for a way to measure the sympathetic nerve activity in a non-invasive and accurate way.

Recently, Robinson et al. have hypothesised that measurements of the sympathetic nerve activity of dermatomes that are innervated via the stellate ganglion, C5, and T1, correlate to the sympathetic activity in the stellate ganglion (SGNA). This hypothesis was proven in a study with dogs, where the researchers found that subcutaneous nerve activity (SCNA) closely correlates with SGNA [9]. Taking it a step further, Doytchinova et al. also found a close correlation between SKNA and SCNA and SGNA. Furthermore, they stated that "it is reasonable to hypothesize that SKNA of the thorax or upper limbs can be used to estimate stellate ganglion nerve activity" [10]. This is a reasonable hypothesis since it is known that sympathetic fibers travel alongside somatosensory fibers and that these postganglionic fibers of the upper limb and thorax synapse in the cervical and stellate ganglia [11–16]. Jiang et al. concluded that it was possible to estimate the sympathetic activity of the stellate ganglion in a representative and non-invasive way by measuring SKNA [17]. With this method, it was shown that in patients with spontaneous tachycardia, 73% of the episodes were preceded by SKNA bursts within 30 seconds of onset [10].

SKNA measurements are an effective way to measure the sympathetic tone in the stellate ganglion but not much is known about the influences of certain variables such as measurement location, BMI, or sex on the SKNA signal. Body fat, estimated with BMI, is a variable of interest because certain so-called adipokines can stimulate the sympathetic nervous system and raise the sympathetic tone. Researchers have also shown that body fat, and especially visceral fat, was associated with sympathetic activation [18,19]. Besides this, it has been determined that postganglionic sympathetic nerve firing rate measured with microneurography in obese subjects was twice that measured in lean subjects [20]. Sex is also an interesting variable because it is known that cardiovascular diseases and their symptoms differ between males and females [21]. Literature also states that the parasympathetic activity in females is higher than in males, whereas sympathetic activity is higher in males. Electrocardiogram (ECG) characteristics and hormones that influence (para)sympathetic activity also differ between the sexes [22,23]. Besides that, no research has yet been done to find the optimal electrode position for SKNA measurements.

To investigate the influence of these variables on the SKNA measurements, we formulated the following research question: In healthy individuals, what is the influence of electrode location, BMI, and sex on skin nerve activity measurements? We hypothesise that a higher BMI and being male will be associated with an increase in average SKNA (aSKNA). There is little evidence concerning the outcomes of different lead positions in SKNA measurements, so we cannot give an informed prediction about the influence of lead positions.

Detailed background information of the anatomy, physiology, and pathology of the sympathetic innervation of the heart can be found in appendix A. An overview of the acronyms and abbreviations used in this article is given in appendix F.

Methods

Study design

A cross-sectional study was started to determine the influence of measurement location, BMI, and sex on the SKNA signal. The SKNA measurements of healthy individuals took place in Medisch Spectrum Twente (MST) and the study was approved by the ethics committee of the faculty of science and technology and the faculty of engineering technology of the University of Twente. All participants were informed with a Dutch information letter, added in appendix D, and gave informed consent.

Study population

47 healthy subjects without any heart condition, neurological condition, or implanted electronic devices were included. The first two exclusion criteria are based on the fact that several heart and neurological conditions have been shown to alter sympathetic activity, thus being a possible covariate in the relationship between BMI or sex and SKNA [4,24–27]. Electronic implants were also excluded because these can interfere with nerve activity, resulting in unusable measurements of SKNA because of its low amplitude. The participants were told to refrain from consuming any stimulating drugs, including caffeine, for 12 hours before the experiment as these stimulants could have been a covariate as well [28].

Measurement design

The Mega Electronics ME6000 Biomonitor (Biomonitor) was used for recording biopotentials. We set a sample frequency of 9600 Hz which makes it possible to record the high-frequency SKNA without morphological disturbance due to aliasing. To determine which lead resulted in the best SNR, six leads were investigated on every subject in two separate measurements. In the first measurement, two leads were placed on the left arm and one on the thorax. For the second measurement, two electrodes were spread across the left arm as far as the equipment allowed, approximately 20 cm, and two more thorax leads were used. See figure 1 for the lead configurations.

Not much is known about the dermatomes corresponding to the different ganglia other than that they are much more extensive and complex compared to the sensory dermatomes. We investigated three leads on the medial side of the left arm when in supination because these C5 and T1 somatosensory dermatomes are hypothetically innervated by sympathetic fibers originating from the stellate ganglion [15,16]. The subjects were placed in a supine position. The measurements started with a minute of laying still, followed by a 15-second Valsalva manoeuvre, followed by another minute of rest and a 15-second Valsalva manoeuvre, and ended with 30 seconds of rest. Valsalva manoeuvre was implemented to make sure that the measurements contained the right signal. In Valsalva manoeuvre the SKNA signal will increase, and thus when no increase is seen, we cannot be certain that the correct signal is measured [10]. The order of measurement was switched in half of the study population. Schematic representations of the measurements and electrode positions can be found in figure 1.

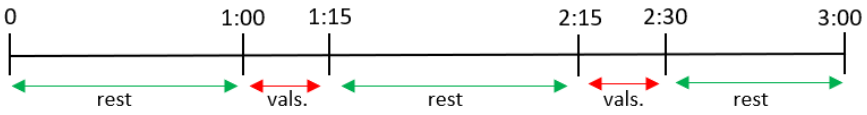

Figure 1a: schematic representation of time management during the measurements, vals. = Valsalva manoeuvre. Time in minutes.

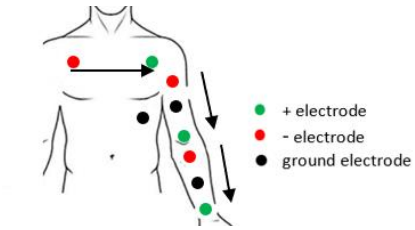

Figure 1b, schematic representation of the lead configuration for the first measurement.

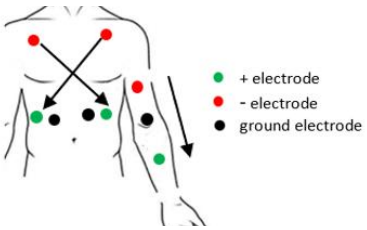

Figure 1c, schematic representation of the lead configuration for the second measurement.

Data analysis

MathWorks MATLAB R2022a software was used for the analysis of the data. To isolate the ECG signal from the raw measurement, a band-pass filter between 0.5 and 150 Hz and a notch filter to eliminate 50 Hz powerline interference were used. A band-pass filter between 500 and 1000 Hz was used to isolate SKNA. The SKNA bursts, which are the result of synchronous conduction of action potentials through peripheral sympathetic nerves, can be absorbed in this background noise due to their small amplitude of only a few microvolts [29–31]. This noise is produced by internal anatomical, biochemical, and physiological factors that take place in the skin, or in the muscles beneath it. This noise has a gaussian distribution because it is stochastic [31–34]. The disadvantage of conventional filters is that it is based on known differences between the frequency spectrum characteristics of noise and signal and that the noise in the frequency range of the signal of interest cannot be removed [35]. This means that filtering either does not completely eliminate noise, or that it is too aggressive in respect of the signal [29]. A wavelet denoising algorithm overcomes this problem because it can remove background Gaussian-distributed noise from the signal spectrum by formulating an accurate threshold [31]. This is because the deterministic neuronal signal only contributes to a few wavelet levels, while the stochastic noise contributes homogeneously to all coefficients and with a lower amplitude. A stationary wavelet denoising algorithm with a Haar mother wavelet, Han et al. level-dependent hard thresholding, and four decomposition levels were used to denoise the filtered SKNA signal. The Haar mother wavelet was used because of its ability to preserve the morphology of the signal and of its higher resulting SNR. A hard thresholding method was used, because this method does not change the spike amplitude after reconstruction, whereas soft thresholding lowers the amplitude [29]. Baldazzi et al. concluded that the most effective threshold for denoising neural signal is a Han et al. level dependent threshold [31,36]. Furthermore, four-level decomposition covers the whole 500 to 1000 Hz band-passed signal. After four levels the approximation level will already be in the frequency range of 0 to 300 Hz. Using more than four levels of decomposition will not be useful because the additional levels would be outside the frequency range of SKNA (500 – 1000 Hz). All these choices are based on literature and our own findings. A more detailed foundation for these choices is elaborated on in appendix B.

The SNR of each lead was then calculated from the average burst activity in the denoised signal and the variance of the eliminated noise, according to equation 1. The average voltage during a certain period was calculated according to equation 2.

$$\mathrm{SNR} = \sqrt{\frac{\mathrm{aSKNA}_{\mathrm{vals}}^2}{\mathrm{var}_{\mathrm{noise}}^2}} \tag{1}$$

with $\mathrm{aSKNA}_{\mathrm{vals}}$ the average voltage during both Valsalva manoeuvres in the denoised signal and $\mathrm{var}_{\mathrm{noise}}$ the variance of the noise that was eliminated by the wavelet denoising method.

$$\mathrm{aSKNA} = \frac{\sum_{i=1}^{\mathrm{N}} \mathrm{SKNA}_i}{\mathrm{N}} \tag{2}$$

with SKNA_i the voltage of sample i and N the total amount of samples.

To analyse the influence of BMI and sex on SKNA measurements, the average voltage during both Valsalva manoeuvres as well as during the rest periods were used as the first two outcome measures. The third outcome measure was the difference in aSKNA between rest and Valsalva manoeuvre intervals as described in equation 3.

$$\Delta\mathrm{aSKNA} = \mathrm{aSKNA}_{\mathrm{vals}} - \mathrm{aSKNA}_{\mathrm{rest}} \tag{3}$$

with $\mathrm{aSKNA}_{\mathrm{vals}}$ the average SKNA during Valsalva and $\mathrm{aSKNA}_{\mathrm{rest}}$ the average SKNA during the rest periods.

Statistical analysis

All outcome measures and independent variables were tested for normality with skewness and kurtosis tests. These tests showed that not all data was normally distributed. Therefore, non-parametric statistical tests were used for most comparisons. The Friedman test was used to determine statistically significant differences in SNR between the six leads. If this difference was found, the Wilcoxon signed-rank test was used for a pairwise comparison of the leads to determine which leads were statistically different. The Kruskal-Wallis test was used to determine the statistical significance of the differences in outcome measures between the BMI and sex groups. When these differences existed, a pairwise comparison between groups was made.

Because BMI was found to be normally distributed in our study population, an independent T-test was used to test for statistically significant differences in BMI between the males and females in the study population. Age was not found to be normally distributed, so to test for statistically significant differences in mean age between males and females, a Mann-Whitney non-parametric test was used.

To determine the statistical significance of the difference in SNR between the six leads, we used the Friedman test, a non-parametric test for repeated measurements. This test is suitable for the comparison of SNR between the leads because all six lead locations were investigated on every subject, the outcome variable (SNR) is continuous, and the data does not have to be normally distributed. The Friedman test only determines whether there is a significant difference between the groups, but it does not determine which leads are significantly different [37]. To determine which leads have a significantly different SNR, a pairwise comparison using the Wilcoxon signed-rank test with Bonferroni adjustment for multiple tests (15 comparisons, $\alpha = \frac{0.05}{15} = 0.00333$) was used. The Wilcoxon signed-rank test was used because it is non-parametric, and it can be used for repeated measurements [38].

To test for the statistical significance of the differences in the three outcome measures ($\mathrm{aSKNA}_{\mathrm{rest}}$, $\mathrm{aSKNA}_{\mathrm{vals}}$, and $\Delta\mathrm{aSKNA}$) in subjects with different BMI, the subjects were divided into BMI groups. These groups were underweight (BMI < 18.5), normal weight (BMI 18.5-25), overweight (BMI 25-30), and obese (BMI > 30). Two sex groups were used: male and female. The Kruskal-Wallis test was used to determine the statistical significance of the differences in outcome measures between the BMI and sex groups. The Kruskal-Wallis test is a non-parametric one-way analysis of variance test. This test was used because it does not assume a normal distribution of the data [39]. As with the Friedman test, because the Kruskal-Wallis test does not identify between which groups the significant difference is located, a pairwise comparison between all groups is used. A Bonferroni adjustment for six comparisons was used.

It is likely that there are interactions between BMI and sex, and one would ideally test for this interaction with a statistical test. However, our data was not normally distributed, so we could not use parametric tests like two-way analysis of variance to test for interaction as these tests assume a normal distribution. Non-parametric tests, on the other hand, cannot test for interaction because these tests are based on differences in mean ranks and do not tell you anything about the absolute size of differences in outcome measures.

A value of $p < 0.05$ was considered a significant result or a Bonferroni adjusted value of $p < 0.003$ for the pairwise comparison between leads. The p-values for the pairwise comparison between BMI groups were adjusted directly.

A detailed description of the statistical tests that were used is given in Appendix C.

Results

Different kinds of artefacts were detected that resulted in unreliable measurements. In some measurements the signal stopped before the end of the measurement. This could have multiple explanations; the main one being that one of the electrodes fell off, or the electrode did not make enough contact with the skin. In some measurements the ECG could not fully be filtered out of the signal, which resulted in noise pulses at a constant frequency, consistent with the ECG. However, this is not the signal we are interested in, causing the baseline activity of the SKNA to be higher than it should be. The last artefact we encountered was a high frequency noise in the raw signal. It is unclear what caused these disturbances, but this signal is not the SKNA signal we are interested in.

We saw that the Valsalva manoeuvres often did not lead to an increase in SKNA signal in the arm leads, while it did lead to an increase in the thorax leads. In the two measurements we always measured an arm lead simultaneously with a thorax lead. For these reasons we decided to exclude measurements when the Valsalva manoeuvre did not lead to an increase in the signal of the thorax lead.

For the visual inspection of the measurements, a signal quality index (SQI) was used to determine whether a measurement should be included or excluded. Two researchers independently applied the SQI, blind for the assessment of the other researcher. If there was a difference between the assessments of the researchers for a certain measurement, this measurement was discussed to make a final decision. Figure 2 shows a flowchart of the SQI and corresponding excluded measurements.

Examples of measurements that were excluded can be found in Appendix E.

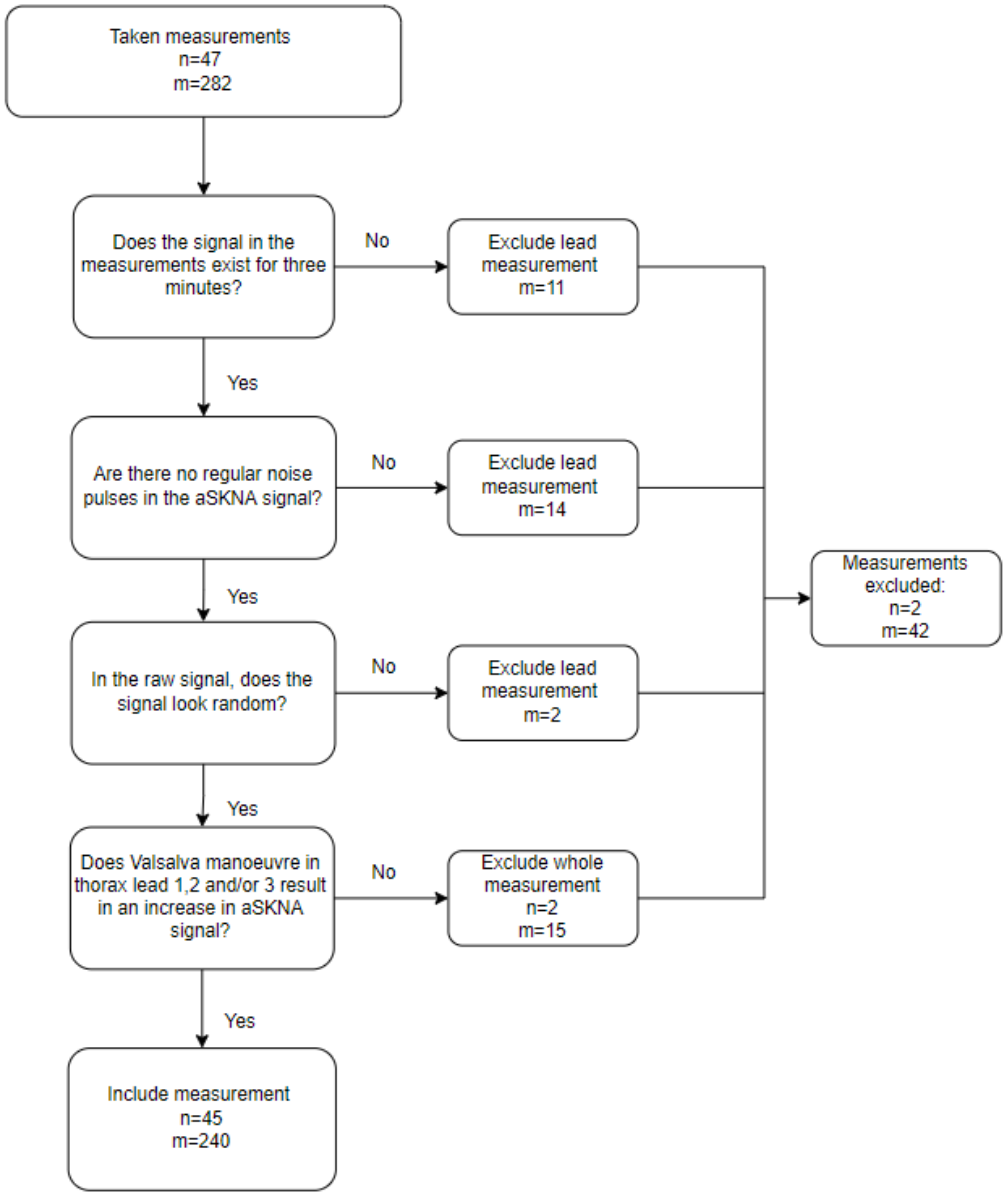

Figure 2: Signal Quality Index; visual analysis for inclusion and exclusion. With n being the number of participants, m being the number of lead measurements

After exclusion based on the SQI, 45 participants and 240 lead measurements were included. Baseline characteristics of this research population can be found in table 1. Additionally graphic display of BMI distribution in the whole research population, and between the sexes can be found in figure 3.

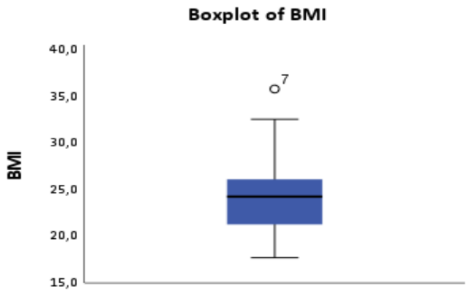

Figure 3a: Boxplot of BMI in total study population

Figure 3b: Boxplot of BMI ordered by sex

Figure 4 shows an example of a successful SKNA measurement with thorax lead III. An increase in SKNA can be seen when the subject performs a Valsalva manoeuvre, while there is little nerve activity being measured during the rest periods. In addition, some residual signal from the R-peaks of the ECG in the raw signal can be seen in the filtered and denoised SKNA signals.

	Female		Male		
	n	*%*	*n*	*%*	*p*
Subjects	26	58	19	42	
BMI (kg/m^2)					
<18,5	2	7,7	0	0	
18,5-25	11	42	14	74	
25-30	9	35	5	26	
>30	4	15	0	0	
Mean (SD)	24.6 (5.0)		23.8 (2.0)		0.475
Age (years)					
Mean (SD)	29 (13)		23.7 (8.1)		0.462

Table 1: Research population characteristics, SD = Standard Deviation.

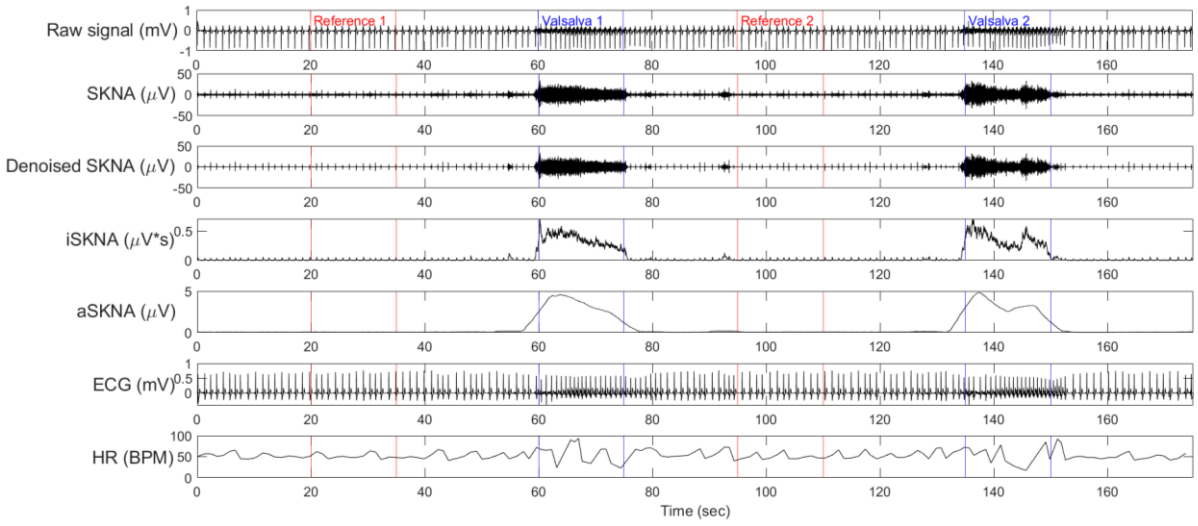

Figure 4: Example of a measurement after signal analysis. From top to bottom: raw signal, band-passed SKNA signal, denoised SKNA signal, intergrated SKNA (iSKNA), aSKNA, ECG and heart rate (HR). The Valsalva periods and reference periods are indicated.

Table 2 shows the mean SNR of the six leads. Using the Friedman test, a statistically significant difference in SNR between the leads was determined as $\chi^2 = 91, p \ll 0.05$. Wilcoxon signed-rank test with Bonferroni adjustment for 15 comparisons ($\alpha = \frac{0.05}{15} = 0.00333$) was used to make a pairwise comparison between the different leads, see table 3.

Lead	Mean SNR (SD)
Forearm	0.84 (0.42)
Upper arm	0.58 (0.34)
Middle arm	0.91 (0.60)
Lead I	1.7 (1.0)
Lead II	2.9 (2.2)
Lead III	3.3 (2.7)

Table 2: Average SNR of all leads

Lead comparison	*p*
Arm leads	
Forearm – Upper arm	< 0.001*
Forearm – Middle arm	0.7
Upper arm – Middle arm	< 0.001*
Thorax leads	
Lead I – Lead II	< 0.001*
Lead I – Lead III	< 0.001*
Lead II – Lead III	0.008
Thorax lead I vs. arm leads	
Lead I - Forearm	< 0.001*
Lead I – Upper arm	< 0.001*
Lead I – Middle arm	< 0.001*
Thorax lead II vs. arm leads	
Lead II – Forearm	< 0.001*
Lead II – Upper arm	< 0.001*
Lead II – Middle arm	< 0.001*
Thorax lead III vs. arm leads	
Lead III – Forearm	< 0.001*
Lead III – Upper arm	< 0.001*
Lead III – Middle arm	< 0.001*

*Table 3: Pairwise comparison of SNR between different leads, $\alpha = 0.003$ after Bonferroni adjustment. $p < 0.003$ is indicated with *.*

Table 4 shows the outcome measures ($\mathrm{aSKNA_{rest}}$, $\mathrm{aSKNA_{vals}}$, and $\Delta\mathrm{aSKNA}$) of the measurements across different BMI groups. Thorax lead II and III were selected to make this comparison because these leads were found to have the highest SNR. Table 5 gives the results of the pairwise comparison of BMI groups.

		Underweight	Normal weight	Overweight	Obese	*p*
Lead II						
	$\mathrm{aSKNA_{rest}}$ (SD) (μV)	0.076 (0.036)	0.22 (0.14)	0.170 (0.090)	0.17 (0.14)	0.2
	$\mathrm{aSKNA_{vals}}$ (SD) (μV)	5.2 (3.5)	2.4 (1.8)	1.09 (0.99)	0.21 (0.17)	0.003**
	ΔaSKNA (SD) (μV)	5.0 (3.3)	2.3 (1.7)	1.00 (0.95)	0.14 (0.23)	0.004**
Lead III						
	$\mathrm{aSKNA_{rest}}$ (SD) (μV)	0.132 (0.033)	0.23 (0.15)	0.166 (0.079)	0.12 (0.14)	0.2
	$\mathrm{aSKNA_{vals}}$ (SD) (μV)	4.00 (0.85)	2.6 (2.1)	1.1 (1.1)	0.23 (0.15)	0.006**
	ΔaSKNA (SD) (μV)	3.77 (0.82)	2.5 (2.0)	1.0 (1.1)	0.20 (0.16)	0.003**

*Table 4: $aSKNA_{rest}$, $aSKNA_{vals}$, and ΔaSKNA in different BMI groups. $p < 0.05$ is indicated with *, $p < 0.01$ is indicated with **.*

		Obese – Overweight	Obese – Normal weight	Obese – Underweight	Overweight – Normal weight	Overweight – Underweight	Normal weight – Underweight
Lead II							
	$\mathrm{aSKNA_{vals}}$ (*p*)	0.7	0.03*	0.02*	0.9	0.4	1
	ΔaSKNA (*p*)	0.9	0.03*	0.03*	0.8	0.3	1
Lead III							
	$\mathrm{aSKNA_{vals}}$ (*p*)	1	0.06	0.08	0.5	0.5	1
	ΔaSKNA (*p*)	1	0.04*	0.08	0.3	0.4	1

*Table 5: Pairwise comparison of aSKNA and ΔaSKNA between different BMI groups, p-values are adjusted with Bonferroni adjustment for 6 comparisons. $p < 0.05$ is indicated with *.*

Table 6 shows $\mathrm{aSKNA_{rest}}$, $\mathrm{aSKNA_{vals}}$ and $\Delta\mathrm{aSKNA}$ in males and in females. Again, thorax lead II and III were selected because they were found to have the highest SNR.

	Male	Female	*p*
Lead II			
aSKNA baseline (SD) (μV)	0.23 (0.13)	0.17 (0.12)	0.02*
aSKNA Valsalva (SD) (μV)	2.8 (1.8)	1.4 (1.8)	0.004**
ΔaSKNA (SD) (μV)	2.6 (1.7)	1.3 (1.7)	0.004**
Lead III			
aSKNA baseline (SD) (μV)	0.23 (0.13)	0.18 (0.12)	0.08
aSKNA Valsalva (SD) (μV)	2.9 (2.0)	1.5 (1.7)	0.01*
ΔaSKNA (SD) (μV)	2.8 (1.9)	1.4 (1.6)	0.005**

*Table 6: $aSKNA_{rest}$, $aSKNA_{vals}$, and ΔaSKNA in males and females. $p < 0.05$ is indicated with *, $p < 0.01$ is indicated with **.*

Discussion

SNR of leads

From table 3 we can conclude that the forearm and middle arm leads had a significantly higher SNR than the upper arm lead, but there was no significant difference in SNR between the forearm and the upper arm leads. All thorax leads had a significantly higher SNR than all arm leads. These results are consistent with previous studies by Doytchinova et al. It became clear that SKNA can be recorded from the thorax of canines and that the morphology and magnitude of the SKNA signal correlated to that of the SGNA. In addition, lead II and III both had a significantly higher SNR than lead I, but there was no significant difference in SNR between lead II and III. It is hard to explain these results because to date, it is generally unknown which skin areas correspond to the various sympathetic ganglia, especially in the upper limbs [12,40]. Multiple studies did show that there is strong evidence that these areas are more extensive and overlapping than the somatosensory dermatomes and that there are large anatomical differences between individuals [15,16]. A possible explanation for the lower SNR in the arm leads is that these areas contain a low sympathetic nerve fiber density. But again, to date, there is no valid data about autonomic nerve fiber densities throughout the body available to confirm this [41]. During visual inspection of the measurements, very few arm lead measurements showed an increase in SKNA during the Valsalva periods. This could indicate that the chosen lead positions did not correspond to dermatomes that are innervated by the stellate ganglion.

aSKNA and BMI

The results in table 4 show that in both lead II and III, there was a statistically significant difference in aSKNA during Valsalva and ΔaSKNA between the different BMI groups, but not in aSKNA during rest. There seems to be a trend between BMI and aSKNA during Valsalva: a higher BMI results in a lower aSKNA during Valsalva and a lower ΔaSKNA. From table 5 we can derive that there was a significantly lower aSKNA during Valsalva and ΔaSKNA in obese subjects when compared to underweight and normal weight subjects in lead II. In lead III, only a significant increase in ΔaSKNA in obese subjects when compared to normal weight subjects was found. These findings contradict our hypothesis, which is based on previous studies that have shown that the amount of white adipose tissue can increase sympathetic activity [18–20]. A deeper look into the SKNA signal is necessary to explain this.

Different subdivisions of sympathetic nerve activity can be distinguished, the two main components being muscle sympathetic nerve activity (MSNA) and skin sympathetic nerve activity (SSNA) [42]. Note that SSNA in the context of microneurography does not refer to the same nerve activity as the skin sympathetic nerve activity (SKNA) that has been investigated in this study. For example, MSNA is inducible by performing a Valsalva manoeuvre or by holding one's breath, while SSNA does not respond to these stimuli [43]. The SKNA that was measured for this study consistently increased during the execution of Valsalva manoeuvres, leading to the hypothesis that SKNA mainly contains MSNA. However, SKNA also shows some asynchronous, seemingly random burst activity, which is more indicative of SSNA [42]. Most likely, SKNA contains both MSNA and SSNA.

A possible explanation for the unexpected correlation between BMI and aSKNA is that the increase of MSNA during Valsalva is damped because subjects with a higher BMI have more subcutaneous fat acting as an isolator between the electrodes and the muscle sympathetic nerves beneath the dermis, while the SSNA does not increase [44]. There was no significant difference in baseline SKNA between the BMI groups.

aSKNA and sex

The results in table 6 show a statistically significant greater aSKNA during rest in males compared to females in lead II, but this was not replicated in lead III. In lead II and III, there was a statistically significant difference in aSKNA during Valsalva and ΔaSKNA between the sexes, with males having higher values. These results are consistent with the effect of different sex hormones on the autonomic nervous system: a greater sympathetic activity in males and a greater parasympathetic activity in females. For example, oestrogen enhances parasympathetic activity and suppresses sympathetic activity. Therefore, sympathetic activity would be higher in males because of lower oestrogen levels, whereas parasympathetic activity would be higher in females [23]. There is also the possibility of men and women differing in autonomic innervation of the thorax. A higher skin sympathetic nerve density would mean a greater aSKNA for males in rest and a higher muscle sympathetic nerve density would mean a greater aSKNA during Valsalva and ΔaSKNA for males [41].

Interaction between BMI and sex

The results of this study could be influenced by interaction between the BMI and sex groups. In our study population, the underweight and obese groups consist of only females. This could have a big impact on the results. For example: if the hypothesis for the influence of sex is correct and women tend to have lower sympathetic activity, the underweight and obese groups will have lower aSKNA measurements. This could be purely a result of the fact that these groups are female, but it could also be the case that the lower values of aSKNA in these groups are caused by the influence of BMI. The correlation between these parameters needs to be clear before any conclusion can be drawn. Because our data is not normally distributed, a statistical test for these interactions does not exist. Therefore, it remains uncertain whether the differences in aSKNA can be explained by sex, BMI or maybe both. In a perfect scenario the measurements would be repeated in a study population where males and females are equally represented in the BMI distribution.

Study limitations

Electrode use

In the individual measurements electrodes were reused, which can have a negative influence on the measurements because of lower adhesion and conduction. However, we tried to eliminate this influence by switching the order of measurement in half of the subjects. It was not investigated whether reused electrodes have an impact on the signal that is obtained.

Valsalva

Real-time assessment of the Valsalva manoeuvre was not possible. Because of this, some of the Valsalva manoeuvres failed. As seen in our SQI, the measurements without a response to the Valsalva manoeuvre were excluded. Additionally, the Valsalva manoeuvre was not objectified in this study. In other studies, a Valsalva manoeuvre was objectified by a manometer which measures the pressure of the Valsalva over time [45,46]. We were not able to measure the pressure and keep it constant during the measurements. Consequently, there is a considerable amount of variance between the measurements in the magnitude of the SKNA signal during Valsalva. Unfortunately, not much is known about the effect of Valsalva pressure on sympathetic activity, so we cannot verify if there is a relationship between pressure magnitude and signal magnitude [47].

Denoising

Baseline SKNA is reduced considerably by our denoising method. It is inevitable that some of the signal of interest is lost due to wavelet denoising, and this is significantly increased in signals with a lower SNR [48]. Due to poor SNR in the baseline of our measurements most of the baseline signal is lost, which means that the calculated aSKNA is lower than in reality. This can be a consequence of calculating the threshold over the whole measurement, which is not optimal because the composition of the signal can vary between baseline and Valsalva. An open-source data base could be used to validate our denoising method and corresponding results, which would make the denoising method more reliable.

ECG in signal

There were still ECG artefacts present in the band-passed SKNA signal, which escaped denoising. This leads to false detection of bursts in the denoised SKNA signal, because the denoising method cannot remove noise with an amplitude higher than the threshold. Due to these limitations, future studies should look at different types of signal processing techniques. An independent component analysis, for example, can be useful to separate different signals, like ECG, electromyography, SKNA and general noise [49]. With a more accurate noise detection mechanism, the accuracy of baseline SKNA would significantly improve.

Generalisability to patient population

Finally, all these limitations come together in the representativity and generalizability of our study. The biggest limitations are caused by the composition of our research population, because the population is not representative for the patient population that is most likely to benefit from the application of SKNA measurements. Sympathetic tone differs between age groups, but the influence of age on SKNA measurements is not yet known, which makes the application of our results on the patient population unreliable [50]. Due to the small sample size and narrow distribution of age in our research population we, unfortunately, could not determine its influence.

Recommendations for further research

Many factors in the design of this study can be improved upon to get more reliable and generalisable results. A more representative research population, for example a broader age distribution, would increase the generalisability of the results. An investigation into the effect of age on SKNA would be worthwhile. Another way to improve on our study design would be to make sure that the BMI distribution in both sex groups is more similar. Furthermore, optimisation of the signal analysis techniques used in this study could improve the usability of baseline SKNA measures, which could provide information about baseline differences caused by patient characteristics. Furthermore, objectifying the Valsalva manoeuvre could eliminate potential confounding of pressure magnitude. Future studies can use our findings to quantify the degree of stellate ganglion block and the corresponding SKNA, by measuring both SGNA and SKNA simultaneously, in patients with recurring VAs.

Conclusion

The aim of this study was to determine the influence of BMI, sex, and electrode location on SKNA measurements. We found that leads II and III resulted in measurements with the highest SNR when compared to lead I and the arm leads. Lead I also had a significantly higher SNR than the arm leads. In addition, we found that obese subjects had a significantly lower aSKNA during Valsalva and ΔaSKNA when compared to underweight and normal weight subjects. No significant differences were found between other BMI groups. Finally, a significantly higher aSKNA in rest as well as during Valsalva and a higher ΔaSKNA were found in males compared to females. All significant differences were noted in lead II, and not all of them were replicated in lead III. It remains unclear whether there was any interaction between sex and BMI that could distort the results. Our findings indicate that measuring the sympathetic tone of the heart by SKNA measurements is best done by placing electrodes on the chest for the highest SNR. In addition, our results have identified some influence of BMI and sex on these measurements. In future research a more representative study population is necessary, with more equal BMI distribution between sex groups and a broader age distribution. Besides that, the signal analysis techniques should be optimised.

References

[1] Centraal Bureau voor de Statistiek. Overledenen; belangrijke doodsoorzaken (korte lijst), leeftijd, geslacht. CBS StatLine 2022. https://opendata.cbs.nl/statline/#/CBS/nl/dataset/7052_95/table (accessed June 23, 2022).

[2] Bhar-Amato J, Davies W, Agarwal S. Ventricular Arrhythmia after Acute Myocardial Infarction: 'The Perfect Storm.' Arrhythmia & Electrophysiology Review 2017;6:134. https://doi.org/10.15420/AER.2017.24.1.

[3] MacIntyre CJ, Sapp JL. Treatment of persistent ventricular tachycardia: Drugs or ablation? Trends in Cardiovascular Medicine 2017;27:506–13. https://doi.org/10.1016/J.TCM.2017.05.004.

[4] Zhang DY, Anderson AS. The Sympathetic Nervous System and Heart Failure. Cardiology Clinics 2014;32:33–45. https://doi.org/10.1016/J.CCL.2013.09.010.

[5] Franciosi S, Perry FKG, Roston TM, Armstrong KR, Claydon VE, Sanatani S. The role of the autonomic nervous system in arrhythmias and sudden cardiac death. Autonomic Neuroscience: Basic and Clinical 2017;205:1–11. https://doi.org/10.1016/J.AUTNEU.2017.03.005.

[6] Ganesh A, Qadri YJ, Boortz-Marx RL, Al-Khatib SM, Harpole DH, Katz JN, et al. Stellate Ganglion Blockade: an Intervention for the Management of Ventricular Arrhythmias. Current Hypertension Reports 2020;22:1–10. https://doi.org/10.1007/S11906-020-01111-8/.

[7] Tian Y, Wittwer ED, Kapa S, McLeod CJ, Xiao P, Noseworthy PA, et al. Effective Use of Percutaneous Stellate Ganglion Blockade in Patients With Electrical Storm. Circ Arrhythm Electrophysiol 2019;12. https://doi.org/10.1161/CIRCEP.118.007118.

[8] Vallbo ÅB, Hagbarth KE, Wallin BG. Microneurography: How the technique developed and its role in the investigation of the sympathetic nervous system. Journal of Applied Physiology 2004;96:1262–9. https://doi.org/10.1152/JAPPLPHYSIOL.00470.2003.

[9] Robinson EA, Rhee KS, Doytchinova A, Kumar M, Shelton R, Jiang Z, et al. Estimating Sympathetic Tone by Recording Subcutaneous Nerve Activity in Ambulatory Dogs. Journal of Cardiovascular Electrophysiology 2015;26:70–8. https://doi.org/10.1111/JCE.12508.

[10] Doytchinova A, Hassel JL, Yuan Y, Lin H, Yin D, Adams D, et al. Simultaneous noninvasive recording of skin sympathetic nerve activity and electrocardiogram. Heart Rhythm 2017;14:25–33. https://doi.org/10.1016/J.HRTHM.2016.09.019.

[11] Visser LH. High-resolution sonography of the superficial radial nerve with two case reports. Muscle Nerve 2009;39:392–5. https://doi.org/10.1002/MUS.21246.

[12] Chakravarthy Marx S, Kumar P, Dhalapathy S, Anitha Marx C, D'Souza AS. Distribution of sympathetic fiber areas of radial nerve in the forearm: an immunohistochemical study in cadavers. Surgical and Radiologic Anatomy 2010;32:865–71. https://doi.org/10.1007/s00276-010-0648-y.

[13] Baron R, Jänig W, With H. Sympathetic and afferent neurones projecting into forelimb and trunk nerves and the anatomical organization of the thoracic sympathetic outflow of the rat. J Auton Nerv Syst 1995;53:205–14. https://doi.org/10.1016/0165-1838(94)00171-F.

[14] Taniguchi T, Morimoto M, Taniguchi Y, Takasaka M, Totoki T. Cutaneous distribution of sympathetic postganglionic fibers from stellate ganglion: A retrograde axonal tracing study using wheat germ agglutinin conjugated with horseradish peroxidase. Journal of Anesthesia 1994;8:441–9. https://doi.org/10.1007/BF02514624.

[15] van Haren FGAM, Driessen JJ, Kadic L, van Egmond J, Booij LHDJ, Scheffer GJ. The relation between skin temperature increase and sensory block height in spinal anaesthesia using infrared thermography. Acta Anaesthesiologica Scandinavica 2010;54:1105–10. https://doi.org/10.1111/J.1399-6576.2010.02298.X.

[16] Moya Amorós J, Prat Ortells J, Morera Abad R, Ramos Izquierdo R, Villalonga Badell R, Ferrer Recuerdo G. Sympathetic dermatomes corresponding to T2 and T3 ganglia. A prospective study of 100 superior thoracic sympathicolytic procedures. Archivos de Bronconeumologia 2003;39:19–22. https://doi.org/10.1016/S0300-2896(03)75309-5.

[17] Jiang Z, Zhao Y, Doytchinova A, Kamp NJ, Tsai WC, Yuan Y, et al. Using skin sympathetic nerve activity to estimate stellate ganglion nerve activity in dogs. Heart Rhythm 2015;12:1324–32. https://doi.org/10.1016/J.HRTHM.2015.02.012.

[18] Smith MM, Minson CT. Obesity and adipokines: effects on sympathetic overactivity. The Journal of Physiology 2012;590:1787–801. https://doi.org/10.1113/JPHYSIOL.2011.221036.

[19] Hillebrand S, de Mutsert R, Christen T, Maan AC, Jukema JW, Lamb HJ, et al. Body fat, especially visceral fat, is associated with electrocardiographic measures of sympathetic activation. Obesity 2014;22:1553–9. https://doi.org/10.1002/OBY.20709.

[20] Grassi G, Seravalle G, Cattaneo BM, Bolla GB, Lanfranchi A, Colombo M, et al. Sympathetic activation in obese normotensive subjects. Hypertension 1995;25:560–3. https://doi.org/10.1161/01.HYP.25.4.560.

[21] Mosca L, Barrett-Connor E, Kass Wenger N. Sex/Gender Differences in Cardiovascular Disease Prevention What a Difference a Decade Makes. Circulation 2011;124:2145. https://doi.org/10.1161/CIRCULATIONAHA.110.968792.

[22] Mieszczanska H, Pietrasik G, Piotrowicz K, McNitt S, Moss AJ, Zareba W. Gender-Related Differences in Electrocardiographic Parameters and Their Association With Cardiac Events in Patients After Myocardial Infarction. American Journal of Cardiology 2008;101:20–4. https://doi.org/10.1016/J.AMJCARD.2007.07.077.

[23] Dart AM, Du XJ, Kingwell BA. Gender, sex hormones and autonomic nervous control of the cardiovascular system. Cardiovascular Research 2002;53:678–87. https://doi.org/10.1016/S0008-6363(01)00508-9.

[24] Zekios KC, Mouchtouri ET, Lekkas P, Nikas DN, Kolettis TM. Sympathetic Activation and Arrhythmogenesis after Myocardial Infarction: Where Do We Stand? Journal of Cardiovascular Development and Disease 2021, Vol 8, Page 57 2021;8:57. https://doi.org/10.3390/JCDD8050057.

[25] Esler M. The Sympathetic System and Hypertension. American Journal of Hypertension 2000;13:S99–105. https://doi.org/10.1016/S0895-7061(00)00225-9.

[26] Pintér A, Cseh D, Sárközi A, Illigens BM, Siepmann T. Autonomic Dysregulation in Multiple Sclerosis. International Journal of Molecular Sciences 2015, Vol 16, Pages 16920-16952 2015;16:16920–52. https://doi.org/10.3390/IJMS160816920.

[27] Kaur D, Tiwana H, Stino A, Sandroni P. Autonomic neuropathies. Muscle & Nerve 2021;63:10–21. https://doi.org/10.1002/MUS.27048.

[28] Corti R, Binggeli C, Sudano I, Spieker L, Hänseler E, Ruschitzka F, et al. Coffee acutely increases sympathetic nerve activity and blood pressure independently of caffeine content role of habitual versus nonhabitual drinking. Circulation 2002;106:2935–40. https://doi.org/10.1161/01.CIR.0000046228.97025.3A.

[29] Zhang Q, Liu YC, Brown L, Shoemaker JK. Challenges and opportunities in processing muscle sympathetic nerve activity with wavelet denoising techniques: Detecting single action potentials in multiunit sympathetic nerve recordings in humans. Autonomic Neuroscience: Basic and Clinical 2007;134:92–105. https://doi.org/10.1016/J.AUTNEU.2007.02.007.

[30] Chowdhury RH, Reaz MBI, bin Mohd Ali MA, Bakar AAA, Chellappan K, Chang TG. Surface Electromyography Signal Processing and Classification Techniques. Sensors (Basel) 2013;13:12431. https://doi.org/10.3390/S130912431.

[31] Baldazzi G, Solinas G, Valle J del, Barbaro M, Micera S, Raffo L, et al. Systematic analysis of wavelet denoising methods for neural signal processing. Journal of Neural Engineering 2020;17:066016. https://doi.org/10.1088/1741-2552/ABC741.

[32] Micera S, Carpaneto J, Raspopovic S. Control of hand prostheses using peripheral information. IEEE Rev Biomed Eng 2010;3:48–68. https://doi.org/10.1109/RBME.2010.2085429.

[33] Rey HG, Pedreira C, Quian Quiroga R. Past, present and future of spike sorting techniques. Brain Research Bulletin 2015;119:106–17. https://doi.org/10.1016/j.brainresbull.2015.04.007.

[34] Lewicki MS. A review of methods for spike sorting: the detection and classification of neural action potentials. Network: Computation in Neural Systems 1998;9:R53–78. https://doi.org/10.1088/0954-898X_9_4_001.

[35] Wiltschko AB, Gage GJ, Berke JD. Wavelet filtering before spike detection preserves waveform shape and enhances single-unit discrimination. Journal of Neuroscience Methods 2008;173:34–40. https://doi.org/10.1016/J.JNEUMETH.2008.05.016.

[36] Han M, Liu Y, Xi J, Guo W. Noise smoothing for nonlinear time series using wavelet soft threshold. IEEE Signal Processing Letters 2007;14:62–5. https://doi.org/10.1109/LSP.2006.881518.

[37] Sheldon MR, Fillyaw MJ, Thompson WD. The use and interpretation of the Friedman test in the analysis of ordinal-scale data in repeated measures designs. Physiotherapy Research International 1996;1:221–8. https://doi.org/10.1002/PRI.66.

[38] Rosner B, Glynn RJ, Lee MLT. The Wilcoxon Signed Rank Test for Paired Comparisons of Clustered Data. Biometrics 2006;62:185–92. https://doi.org/10.1111/J.1541-0420.2005.00389.X.

[39] Chan Y, Walmsley RP. Learning and Understanding the Kruskal-Wallis One-Way Analysis-of-Variance-by-Ranks Test for Differences Among Three or More Independent Groups. Physical Therapy 1997;77:1755–61. https://doi.org/10.1093/PTJ/77.12.1755.

[40] Keplinger M, Marhofer P, Moriggl B, Zeitlinger M, Muehleder-Matterey S, Marhofer D. Cutaneous innervation of the hand: clinical testing in volunteers shows high intra- and inter-individual variability. British Journal of Anaesthesia 2018;120:836–45. https://doi.org/10.1016/J.BJA.2017.09.008.

[41] Glatte P, Buchmann SJ, Hijazi MM, Illigens BM-W, Siepmann T. Architecture of the Cutaneous Autonomic Nervous System. Frontiers in Neurology 2019;10:970. https://doi.org/10.3389/fneur.2019.00970.

[42] Greaney JL, Kenney WL. 50 Years of Microneurography: Insights into Neural Mechanisms in Humans: Measuring and quantifying skin sympathetic nervous system activity in humans. Journal of Neurophysiology 2017;118:2181. https://doi.org/10.1152/JN.00283.2017.

[43] Macefield VG. Sympathetic microneurography. Handbook of Clinical Neurology 2013;117:353–64. https://doi.org/10.1016/B978-0-444-53491-0.00028-6.

[44] Kuiken TA, Lowery MM, Stoykov NS. The effect of subcutaneous fat on myoelectric signal amplitude and cross-talk. Prosthetics and Orthotics International 2003;27:48–54. https://doi.org/10.3109/03093640309167976.

[45] Monge García MI, Gil Cano A, Díaz Monrové JC. Arterial pressure changes during the Valsalva maneuver to predict fluid responsiveness in spontaneously breathing patients. Intensive Care Medicine 2009;35:77–84. https://doi.org/10.1007/S00134-008-1295-1.

[46] Cooke WH, Carter JR, Kuusela TA. Muscle sympathetic nerve activation during the Valsalva maneuver: interpretive and analytical caveats. Aviat Space Environ Med 2003;74:731–7.

[47] Low PA. Valsalva Maneuver. Encyclopedia of the Neurological Sciences 2014:591–2. https://doi.org/10.1016/B978-0-12-385157-4.00517-0.

[48] Brychta RJ, Shiavi R, Robertson D, Diedrich A. Spike detection in human muscle sympathetic nerve activity using the kurtosis of stationary wavelet transform coefficients. J Neurosci Methods 2007;160:359. https://doi.org/10.1016/J.JNEUMETH.2006.09.020.

[49] Li ZY, Liu SR, Xie ZX, Wang W. Using independent component analysis to research heart rate variability. Conf Proc IEEE Eng Med Biol Soc 2005;2005:5532–5. https://doi.org/10.1109/IEMBS.2005.1615737.

[50] Abhishekh HA, Nisarga P, Kisan R, Meghana A, Chandran S, Trichur Raju, et al. Influence of age and gender on autonomic regulation of heart. Journal of Clinical Monitoring and Computing 2013;27:259–64. https://doi.org/10.1007/S10877-012-9424-3.

[51] Richerson GB. The Autonomic Nervous System. In: Boron WF, Boulpae EL, editors. Medical Physiology. 3rd ed., Elsevier; 2017, p. 334–52.

[52] Moore KL, Dalley AF, Agur AMR. Nerves in root of neck. Clinically Orientated Anatomy. 8th ed., Philadelphia: Wolters Kluwer; 2018, p. 1025–6.

[53] Kawashima T. The autonomic nervous system of the human heart with special reference to its origin, course, and peripheral distribution. Anatomy and Embryology 2005;209:425–38. https://doi.org/10.1007/s00429-005-0462-1.

[54] Kawashima T. The autonomic nervous system of the human heart with special reference to its origin, course, and peripheral distribution. Anatomy and Embryology 2005;209:425–38. https://doi.org/10.1007/s00429-005-0462-1.

[55] Schwartz PJ. Cardiac sympathetic denervation to prevent life-threatening arrhythmias. Nature Reviews Cardiology 2014 11:6 2014;11:346–53. https://doi.org/10.1038/nrcardio.2014.19.

[56] Fudim M, Boortz-Marx R, Ganesh A, Waldron NH, Qadri YJ, Patel CB, et al. Stellate ganglion blockade for the treatment of refractory ventricular arrhythmias: A systematic review and meta-analysis. J Cardiovasc Electrophysiol 2017;28:1460–7. https://doi.org/10.1111/JCE.13324.

[57] Ajijola OA, Yagishita D, Reddy NK, Yamakawa K, Vaseghi M, Downs AM, et al. Remodeling of stellate ganglion neurons after spatially targeted myocardial infarction: Neuropeptide and morphologic changes. Heart Rhythm 2015;12:1027–35. https://doi.org/10.1016/J.HRTHM.2015.01.045.

[58] Zaglia T, Mongillo M. Cardiac sympathetic innervation, from a different point of (re)view. The Journal of Physiology 2017;595:3919–30. https://doi.org/10.1113/JP273120.

[59] Mtui E, Gruener G, Dockery P. Automonic nervous system and visceral efferents. Fitzgerald's Clinical Neuroanatomy and Neuroscience. 7th ed., Elsevier; 2016.

[60] Everett TH, Doytchinova A, Cha YM, Chen PS. Recording Sympathetic Nerve Activity from the Skin. Trends Cardiovasc Med 2017;27:463. https://doi.org/10.1016/J.TCM.2017.05.003.

[61] Bootsma M, Swenne CA, van Bolhuis HH, Chang PC, Cats VM, Bruschke AVG. Heart rate and heart rate variability as indexes of sympathovagal balance. Am J Physiol 1994;266. https://doi.org/10.1152/AJPHEART.1994.266.4.H1565.

[62] Bayles RG, Olivas A, Denfeld Q, Woodward WR, Fei SS, Gao L, et al. Transcriptomic and neurochemical analysis of the stellate ganglia in mice highlights sex differences. Scientific Reports 2018;8:8963. https://doi.org/10.1038/s41598-018-27306-3.

[63] Qiao S, Torkamani-Azar M, Salama P, Yoshida K. Stationary wavelet transform and higher order statistical analyses of intrafascicular nerve recordings. Journal of Neural Engineering 2012;9:056014. https://doi.org/10.1088/1741-2560/9/5/056014.

[64] Johnstone IM, Silverman BW. Wavelet Threshold Estimators for Data with Correlated Noise. Journal of the Royal Statistical Society: Series B (Statistical Methodology) 1997;59:319–51. https://doi.org/10.1111/1467-9868.00071.

[65] Donoho DL, Johnstone JM. Ideal spatial adaptation by wavelet shrinkage. Biometrika 1994;81:425–55. https://doi.org/10.1093/BIOMET/81.3.425.

[66] Donoho DL. De-Noising by Soft-Thresholding. IEEE Transactions on Information Theory 1995;41:613–27. https://doi.org/10.1109/18.382009.

[67] Diedrich A, Charoensuk W, Brychta RJ, Ertl AC, Shiavi R. Analysis of raw microneurographic recordings based on wavelet de-noising technique and classification algorithm: Wavelet analysis in microneurography. IEEE Transactions on Biomedical Engineering 2003;50:41–50. https://doi.org/10.1109/TBME.2002.807323.

[68] Messer SR, Agzarian J, Abbott D. Optimal wavelet denoising for phonocardiograms. Microelectronics Journal 2001;32:931–41. https://doi.org/10.1016/S0026-2692(01)00095-7.

[69] Blanca MJ, Arnau J, López-Montiel D, Bono R, Bendayan R. Skewness and Kurtosis in Real Data Samples. Methodology 2013;9:78–84. https://doi.org/10.1027/1614-2241/a000057.

[70] Cain MK, Zhang Z, Yuan K-H. Univariate and multivariate skewness and kurtosis for measuring nonnormality: Prevalence, influence and estimation. Behavior Research Methods 2017;49:1716–35. https://doi.org/10.3758/s13428-016-0814-1.

[71] Kim H-Y. Statistical notes for clinical researchers: assessing normal distribution (2) using skewness and kurtosis. Restorative Dentistry & Endodontics 2013;38:52. https://doi.org/10.5395/RDE.2013.38.1.52.

[72] McKnight PE, Najab J. Mann-Whitney U Test. The Corsini Encyclopedia of Psychology 2010:1–1. https://doi.org/10.1002/9780470479216.CORPSY0524.

[73] Nachar N. The Mann-Whitney U: A Test for Assessing Whether Two Independent Samples Come from the Same Distribution. Tutorials in Quantitative Methods for Psychology 2008;4:13–20. https://doi.org/10.20982/TQMP.04.1.P013.

Appendix A: Anatomy, physiology, and pathology of the sympathetic innervation of the heart

Anatomy and physiology

General anatomy of the autonomic nervous system

The innervation of the autonomic nervous system from the spinal cord to the target organ consist of two neurons. These are the preganglionic neuron and the postganglionic neuron. The cell bodies of sympathetic preganglionic neurons are in the thoracic and lumbar spinal cord, between levels T1 and L3. From there, sympathetic signalling routes pass through sympathetic/paravertebral ganglions. In the paravertebral ganglion there are three routes that a signal can take:

1. Synapse in the ganglion and continue via a postganglionic neuron.
2. Travel through the sympathetic chain to neighbouring ganglia via a sympathetic trunk and synapse in that ganglion.
3. Leave the ganglion via the same preganglionic neuron and synapse in one of the prevertebral ganglia.

Sympathetic paravertebral and prevertebral ganglia are located close to the spinal cord, so sympathetic preganglionic neurons are quite short. The superior cervical, middle cervical, and stellate (cervicothoracic) ganglia, important in the innervation of the heart, are paravertebral ganglia. On the other hand, parasympathetic preganglionic neurons are quite long, because the ganglia where they synapse are located close to their target organ. Therefore, the parasympathetic postganglionic neurons are short. The cell bodies of the preganglionic neurons of the parasympathetic system are in the craniosacral divisions of the central nervous system. Most of the parasympathetic preganglionic cell bodies are in the medulla, pons, and midbrain. From here the parasympathetic fibres form a couple of cranial nerves. The parasympathetic control of the heart is provided by the vagus nerve (CN X) [51].

Anatomy of the innervation of the heart

The innervation of the human heart is provided by the cardiac autonomic nervous system. The system consists of two separate pathways, the parasympathetic and sympathetic nerve pathway. The heart is innervated by the cervical portion of the sympathetic chain anterolateral to the vertebral column. It consists of four cervical sympathetic ganglia; the superior cervical ganglion, middle cervical ganglion, vertebral ganglion, and stellate ganglion [52]. The stellate ganglion consists of the inferior cervical ganglion and the first thoracic ganglion and is found in most individuals. The superior and stellate ganglion are consistent throughout most people, but the middle and vertebral ganglion differ in size, position and communicating branches of the spinal nerves. All ganglia are connected with different branches of the spinal nerves. The superior cervical ganglion is connected with C1-C3. The middle cervical ganglion is variable but is usually connected with C3-C6. The inferior cervical ganglion is part of the stellate ganglion and has a range of C5-T3 but is always connected with C8 and T1 [53].

The ganglia give rise to numerous sympathetic nerves that are connected with the heart. The superior cervical, middle cervical and inferior cervical/stellate ganglia respectively give rise to the superior, middle, and inferior cardiac nerve. These nerves travel along the path of the brachiocephalic trunk, common carotid, and subclavian arteries to the cardiac plexus where they are joined by branches of the parasympathetic nerves [53].
The parasympathetic stimulation originates from the 10th cranial nerve, the vagus nerve. The vagus nerve gives rise to different cardiac branches. These branches are named after their origin and are the superior cardiac branch, inferior cardiac branch, and the thoracic cardiac branch. They all end in a part of the cardiac plexus [54].

Stellate ganglion

The stellate ganglion is located anterior to the C7 or T1 vertebra, superior to the neck of the first rib, and posterior to the origin of the vertebral artery. It is called “stellate” because of its star-like shape [6,52].
Most ganglia receive presynaptic fibres through the superior spinal nerves (T1-T5) and their associated white rami communicantes which ascend to the ganglia through the sympathetic chain [52]. Sympathetic postganglionic nerves provide efferent innervation to the heart, upper extremity, neck, and face [6]. Even

though the stellate ganglia are bilateral, they have different effects on the heart. Studies show that the left stellate ganglion has a bigger share of the sympathetic tone than the right [55]. Therefore, a stellate ganglion block (SGB) is mainly performed unilaterally left-sided [7,56]. However, myocardial damage can lead to remodelling of the ganglia [6]. For example, myocardial infarction leads to an increase in the number of neurons and synaptic density 5 weeks after the incident. This is an argument for the use of bilateral SGB [57].

Cardiac sympathetic nervous innervation

The myocardium is extensively innervated by sympathetic and parasympathetic nerves (SNs and PNs, respectively). Every cardiomyocyte (CM) contacts multiple neuronal processes, including SNs. SNs have multiple effects on CMs, both in rest and in fight or flight situations. SNs increase chronotropy by secreting noradrenaline (NA) and stimulating β-adrenoceptors in CMs of the sinoatrial node and they increase inotropy by stimulating β-adrenoceptors in contracting CMs of the myocardium. SNs are responsible for the maintenance and growth of CMs as well. SNs also work in tandem with PNs to regulate heart rate on a beat-to-beat basis. This regulation of heart rate has a remarkably high temporal resolution and is based on factors such as respiratory rate, hormones, hemodynamic reflexes, and temperature. Because the temporal resolution of neuronal regulation of heart rate is so high, and the interstitial space is not favourable to the exchange of NA, it is hypothesised that there must be a direct contact between neurons and CMs, and secretion of NA must take place in the intracellular space as opposed to the interstitial space [58].

The sinoatrial node on the right side of the body is mainly innervated by two right-sided sets of autonomic neurons, while the atrioventricular node is on the left side and receives left sided sets of autonomic neurons. The sinoatrial node is highly responsive to emotions originating from the right hemisphere. However, lateralisation of cardiovascular innervation has not yet been fully resolved [59].

Pathology

In patients suffering from HF or MI, the autonomic innervation of the heart is often disturbed, including an increase in sympathetic tone. The increase in sympathetic stimulation in HF is due to an increase in excitation and a decrease in inhibition of the hypothalamus and medulla, which regulate sympathetic tone. This increase in stimulation is partly meant to compensate physiological changes caused by HF and is partly a pathological mechanism. One of the mechanisms of increased excitation is activation of the renin-angiotensin aldosterone system in the brain. Angiotensin II stimulates Angiotensin II type I receptors in the hypothalamus and medulla, which in turn increases sympathetic tone. Aldosterone further increases this effect by causing an increase in expression of Angiotensin II type I receptors in the hypothalamus. Inflammatory cytokines in the brain also play a role in the decreased inhibition of the sympathetic regulation centres [4].

The increased sympathetic stimulation of the heart in HF patients has several effects. The SNs secrete more NA, which in the short term causes the heart to increase inotropy and chronotropy. Sustained stimulation by SNs, however, causes CMs to desensitise to NA, due to a decrease in expression of β-adrenoceptors and a less effective signalling pathway downstream of these receptors. This desensitisation causes the CMs to be less responsive to stimulation from the CNS, and increases apoptosis, leading to progression of HF [4].

The increase in sympathetic tone seen in patients with HF or MI, in combination with a change in parasympathetic stimulation, can lead to several types of cardiac arrhythmias. For example, a simultaneous increase in sympathetic and parasympathetic stimulation to the heart can increase the risk of atrial fibrillation. An increase in sympathetic tone has also been shown to precede instances of ventricular tachycardia [5].

As is shown above, sympathetic tone is important in cardiac arrhythmias. There are different ways to estimate cardiac autonomic nerve activity. Common ways to measure autonomic nerve activity are measuring the heartrate variability or measuring the nerve activity by means of microneurography [8]. However, these methods lack in a couple of ways because they are either too invasive, or they do not represent the actual sympathetic tone. That is why there is a need to measure the sympathetic nerve activity in a non-invasive and representative way.

In the last few years, researchers discovered that SGNA can be measured by skin measurements on the chest or the arm, because several SNs that innervate the skin of the chest and arms run via the stellate ganglion and are activated simultaneously with the stellate ganglion [60]. In a study with ambulatory dogs, it was shown that SCNA measurements and SGNA closely correlate with each other [9]. The researchers then took it a step further by measuring SKNA and comparing these to SGNA and SCNA. They concluded that the SKNA was also closely correlated with SGNA, which makes it possible to estimate the sympathetic tone of the heart in a representative and non-invasive way [17].

Effects of patient characteristics on sympathetic activity

Influence of body fat on sympathetic activity

It has been shown that the amount of body fat can influence sympathetic activity. Smith and Minson determined that obesity can stimulate the sympathetic nervous system by secretion of a couple of different so-called 'adipokines.' These adipokines may activate the neural sympathetic nervous system [18]. Grassi et al. found that postganglionic sympathetic nerve firing rate in obese subjects was twice of that seen in lean subjects. Hillebrand et al. have that body fat, and especially visceral fat, is associated with sympathetic activation. They concluded that body fat was associated with different measures of sympathetic activity. None of the subjects had any cardiovascular diseases. A big limitation of this study was that there was not a direct measure to measure sympathetic activity. They used heart rate and heart rate variability to estimate the sympathetic activation [19]. These have been shown to be dependable parameters to measure autonomous function. However, in patients with heart conditions these parameters are not reliable [61]. SKNA can be a reliable measure, because it measures the sympathetic activity from the stellate ganglion, but we need to investigate the effect of body fat on these SKNA measurements. Body fat is known to raise the sympathetic activity and therefore we expected to see higher baseline values of sympathetic activity in subjects with a higher BMI.

Influence of sex on sympathetic activity

The influence of sex on sympathetic activity remains unclear. However, it is known that ECG characteristics are not the same in men and women. For example, women have faster heart rates, the QRS duration is shorter and the QTc is longer than in males [22]. Besides this, there is substantial evidence that different hormones in males and females also influence nerve activity. Oestrogen enhances parasympathetic activity. Therefore, sympathetic activity would be higher in males, whereas parasympathetic activity would be higher in females [23]. In mice, it has also been found that the composition and gene expression in the stellate ganglion were different for males and females. This could mean that innervation of target tissues differs between the sexes [62]. Because of this, we investigated the influence of sex on the SKNA measurements, where we expected to see higher levels of sympathetic activity in males.

Appendix B: Wavelet denoising

Noise

The sympathetic nervous system produces burst discharge patterns by conducting synchronous action potentials through multiple axons at a time. This results in a small potential difference of a couple of microvolts that can be measured on the skin [29]. When we took our first test measurements, we saw that the raw SKNA signal contained a significant amount of high frequency noise. The character of the SKNA signal, which originates from synchronous conduction of action potentials (bursts) through peripheral sympathetic nerves resulting in spikes, is invisible due to this background noise. This results in an often exceptionally low SNR [29–31]. The following paragraph will explain the several types of noise and conventional ways to reduce their impact and eventually we will discuss a signal analysis technique called the wavelet transform to denoise our signal.

Electronical equipment produces a certain amount of noise by itself, this is called inherent noise. Another example of electromagnetic noise is a 50 Hz radiation from the electricity network. This noise is the result of our body constantly being exposed to electric and magnetic radiation. Since our bodies function as antennae, stray currents are generated due to impedance difference between the electrodes [30]. The use of a notch filter attenuates this 50 Hz noise.

Lead I, II and III from our protocol are similar to the conventional Einthoven leads and are designed to measure cardiac activity. Thus, the raw SKNA signal contains a big share of ECG signal, which is noise because we are initially not interested in this type of signal when analyzing the SKNA. The use of a 150 Hz high pass filter is an effective way to attenuate this noise [30].

When a subject performs a Valsalva manoeuvre, there is a possibility that one or more cables connecting the electrodes with the Biomonitor, move resulting in a motion artefact. Several causes exist for this artefact, for example the movement between the electrodes and the peripheral nerve. These artefacts have a frequency range of one up to ten Hz and can be attenuated by a twenty Hz high pass filter [30].

Internal anatomical, biochemical, and physiological factors that take place in the skin or in the muscles beneath it produce internal noise, often with an amplitude greater than an action potential [32–34]. Examples of this are muscle activity and other distant neuronal populations [31].

The downside of all these traditional filter methods is that the parameters are chosen based on known differences between the spectral characteristics of noise and signal, and that the noise in the frequency range of the signal cannot be removed [35]. This means that filtering is not ideal or that it is too aggressive in respect of the signal [29].

Wavelet transform & denoising

There is a signal analysis technique to overcome the problems that are associated with conventional filtering methods called the wavelet transform (WT). With this WT it is possible to reduce background Gaussian-distributed noise from the signal spectrum. The superiority of the WT compared to traditionally filter methods has already been proven [31,35]. The WT expresses the signal in the time-frequency domain as a sum of temporally scaled and shifted versions of a base wavelet function [29,31].These so-called coefficients are divided in approximation and detail coefficients. The detail coefficients are the result of a convolution between the signal and a scaled wavelet. The wavelet transform can be described mathematically by equation 4. Equation 5 expresses the dilated and shifted versions of the mother wavelet with the conditions that *a* is any positive number and *b* is any real number [31].

$$Wf(a,b) = \int y(t)\varphi *_{a,b} (t)\, dt \quad (4)$$

$$\varphi_{a,b}(t) = \frac{1}{\sqrt{a}}\varphi\left(\frac{t-b}{a}\right) \quad (5)$$

If a and b are chosen to be discrete parameters, then the continuous wavelet transform (CWT) of equation 4 becomes a discrete wavelet transform (DWT). If $a = 2^j$ and $b = k2^j$ where k and j are integers, the decomposition of the signal is dyadic. Parameter j corresponds to the level of decomposition. Computing the

DWT is a useful denoising strategy. The algorithm can be seen as a "filtering tree" where at each level the signal is high-passed through convolution with the defined wavelet. This process is repeated up to the desired decomposition level. The highest sub-band, containing the approximation coefficients, includes frequencies ranging from 0 to $f_n/2^j$ with f_n denoting the Nyquist frequency. The lowest sub-band contains the Nyquist frequency.

A big drawback of the DWT is down sampling of the data with each level of decomposition. This results in distorted or missing spikes. The stationary wavelet transform (SWT) is a type of DWT that overcomes this problem by upsampling of the data from the previous decomposition level, maintaining the time resolution of the original signal [31].

The detail coefficients are thresholded before the signal is reconstructed. This means that any detail coefficient below the threshold is set to zero [29]. The common threshold depends on the standard deviation of the noise in the raw data with the assumption that the noise has a normal distribution. However, noise can be unstructured due to low-level nerve activity of remote nerves [63]. This means that the standard deviation of the noise may be diverse through the levels [64]. Equation 6 calculates the standard deviation for each level "as the 75th percentile of the median absolute deviation calculated for the j-level detail coefficients cDj" [31].

$$\sigma_j = \frac{median(|cD_j|)}{0.6745} \tag{6}$$

There are several ways to define a threshold and a thresholding method. The two most widely used methods are soft and hard thresholding [65,66]. Hard thresholding sets all detail coefficients of a certain level to zero if it is less than the defined threshold and leaves the other coefficients untouched, whereas soft thresholding also subtracts the threshold value from all coefficients higher than the threshold [31]. We used the hard thresholding method because this does not change the spike amplitude after reconstruction, whereas soft thresholding lowers the amplitude [29]. Besides this, hard thresholding results in a higher SNR and it loses less true neural signal than soft thresholding. This last fact can be deduced by comparing a Q-Q plot of the eliminated noise via hard and soft thresholding, respectively. Stochastic noise has a normal distribution and the residuals obtained via hard thresholding correlate better to $y = x$ than the residuals obtained via soft thresholding [67]. Baldazzi et al. determined the most effective threshold for denoising neural signal to be the Han et al. level dependent threshold [31,36]. The threshold is defined in equation 7 where L is the highest decomposition level, N is the sample and j is the level.

$$\theta_j \begin{cases} \sigma_j\sqrt{2\ln(N)} \;\; if\; j = 1 \\ \frac{\sigma_j\sqrt{2\ln(N)}}{\ln(j+1)} \;\; if\; 1 < j < L \\ \frac{\sigma_j\sqrt{2\ln(N)}}{\sqrt{j}} \;\; if\; j = L \end{cases} \tag{7}$$

In addition, the choice of the mother wavelet and the decomposition level influences the denoising quality. Literature states that the wavelet shape must resemble the signal of interest. In an ideal situation, the wavelet matches the signal so that one coefficient represents the whole signal [68]. This resulted in a widespread use of the Symlets 7 (Sym7) and Daubechies 4 (Db4) wavelets. However, these wavelets had a negative influence on the neural spike morphology. The Haar mother wavelet and Han et al. hard thresholding result in the best SNR and morphological conservativeness [31].

Review of our data

To investigate the choices we made about thresholding and to evaluate the choice of levels of decomposition and the mother wavelet, we reviewed the data ourselves by looking at the Q-Q plots of the residuals of the SKNA signal. The residuals represent the noise that has been filtered via the wavelet denoising method. We compute the residuals by taking the original SKNA signal and subtracting the denoised SKNA signal. The Q-Q plots can tell us a lot about the way how the residuals are distributed. In the perfect situation, the filtered stochastic noise has a normal distribution. The central limit theorem tells us that when a lot of different noise sources are added up, the noise will be normally distributed, meaning that the residuals in the Q-Q plots will follow the line $y = x$.

To start, we evaluated the different thresholding methods; thresholding with or without a level-dependent standard deviation. The difference is that the SDs in the level-dependent method are calculated on the detailed coefficients per level instead of over the whole data. The wavelet decomposition functions as a filter bank, which means that the standard deviation is calculated over a frequency band. The raw signal contained ECG signal, which resulted in a great error when we calculated the SD without a level-dependent threshold. Therefore, we used the band-passed SKNA signal to calculate the SD. Secondly, we evaluated the different levels of decomposition. And lastly, we investigated the choice of the mother wavelet.

Thresholding

Comparing the residuals in figure 5 and figure 6, we can see that level-dependent thresholding removes more signal than non-level-dependent thresholding. In the case of level-dependent thresholding, the signal will always be filtered in a consistent way. The level-dependent SD method will therefore filter the signal in the most uniform way, so this will be our choice. This choice is consistent with the literature.

Decomposition levels

We set the approximation coefficients to zero, which leads to the SWT functioning as a high-pass filter with the highest frequency of the approximations as the cut-off [31]. Low levels of decomposition will eliminate a significant portion of the signal if we set the approximation coefficients to zero. For example, with a sample frequency of 9600 Hz, two levels of decomposition will result in an approximation level with a maximum frequency of 1200 Hz. When setting the approximation coefficients to zero it will throw away all of the 500-1000 Hz SKNA signal. The maximum frequency of the approximation coefficients obtained by three decomposition levels is 600 Hz which means that the signal between 500-600 Hz is not taken into account. Four decomposition levels will cover the whole 500-1000 Hz spectrum so most of the signal is maintained. After four levels of decomposition, the approximation level will already be in the frequency range of 0-300 Hz. Using more than four levels of decomposition will not be useful because the approximation level is outside the frequency range of SKNA. So we will use four levels of decomposition to maintain all the SKNA signals.

Mother wavelet

In figure 5, the residuals obtained using a threshold with level-dependent SD and with different mother wavelets are displayed. All wavelets at four levels of decomposition seem to filter the noise equally over the whole timeframe because the residuals look equal in morphology. In figure 6, the residual obtained with different mother wavelets, but without a level-dependent SD are displayed. This figure shows that at four levels of decomposition, the morphology of the noise is different between wavelets. In the Q-Q plots in figures 9 and 10 we can see how the noise is distributed in different periods of the measurement. While doing the Valsalva manoeuvre (figure 9), there is a thin-tailed Q-Q plot at every level and with every wavelet, which means that a small amount of noise is passed into the denoised signal. In the Valsalva period, this is not of any harm, because the nerve activity is much greater in magnitude than the noise. At rest, you want to filter the noise in the most accurate way possible, so that only the signal remains after the denoising. At rest (figure 10), the residuals at four levels of decomposition show a fat-tailed Q-Q plot, which overestimates the noise and which filters some of the nerve activity out of the signal. All wavelets seem to perform the same in rest and Valsalva, so we chose the Haar mother wavelet based on the literature.

Figure 7 shows Q-Q plots of the residuals at different levels of decomposition and with different wavelet, using a threshold with level-dependent SD. Figure 8 shows Q-Q plots of the residuals at different levels of decomposition and with different wavelet, using a threshold with level-dependent SD.

In summary, based on our own findings and on the literature, we denoise our SKNA signal with the SWT with a Han et al. level-dependent hard thresholding method, Haar mother wavelet and four decomposition levels.

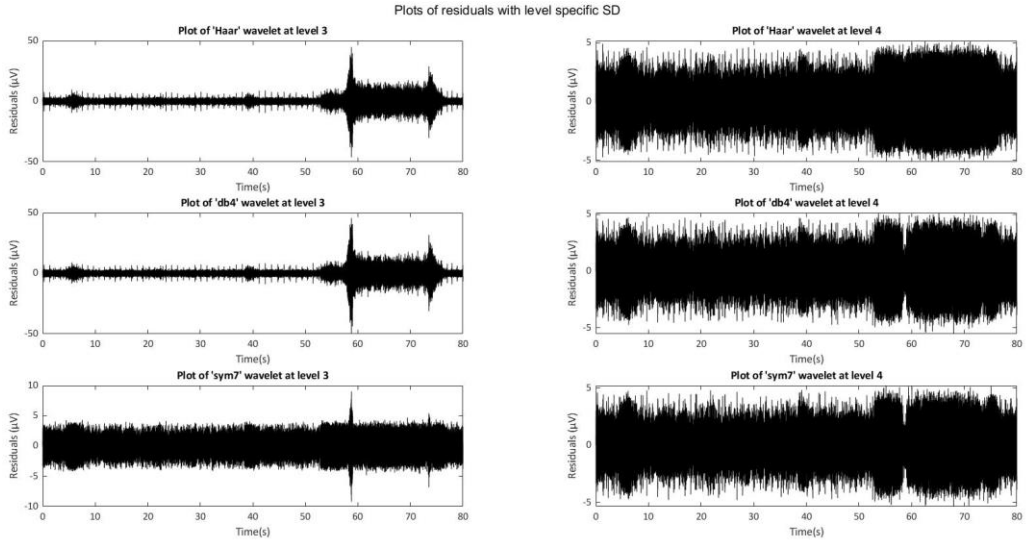

Figure 5: Plots of residuals at different levels of decomposition and with different wavelets, with a threshold with level-dependent SD. Time interval 0 – 80s.

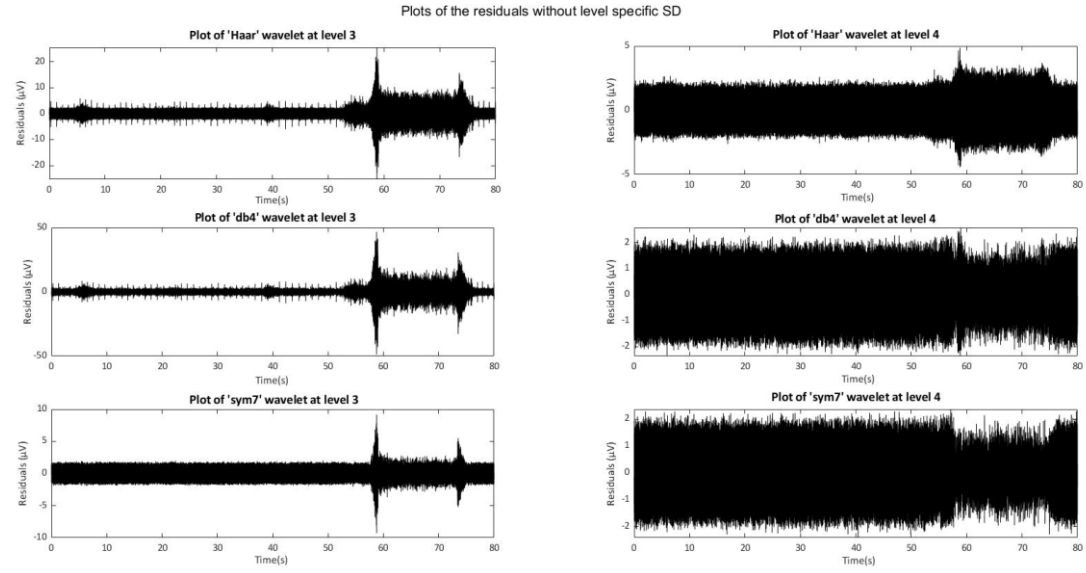

Figure 6: Plots of residuals at different levels of decomposition and with different wavelets, with a threshold with non-level-dependent SD. Time interval 0 – 80s.

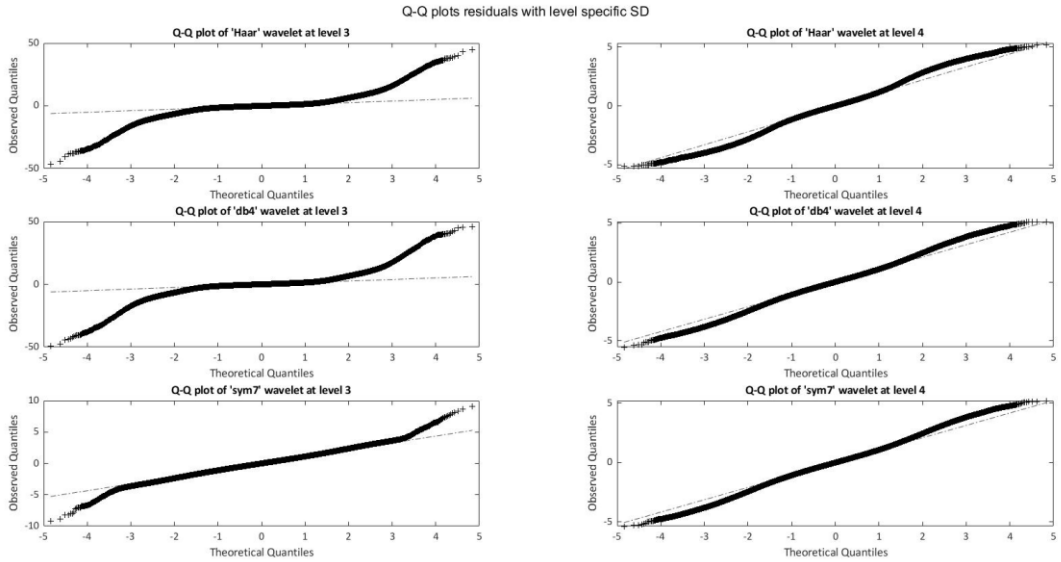

Figure 7: Q-Q plots of residuals at different levels of decomposition and with different wavelets, with a threshold with level-dependent SD. Time interval 0 – 80s.

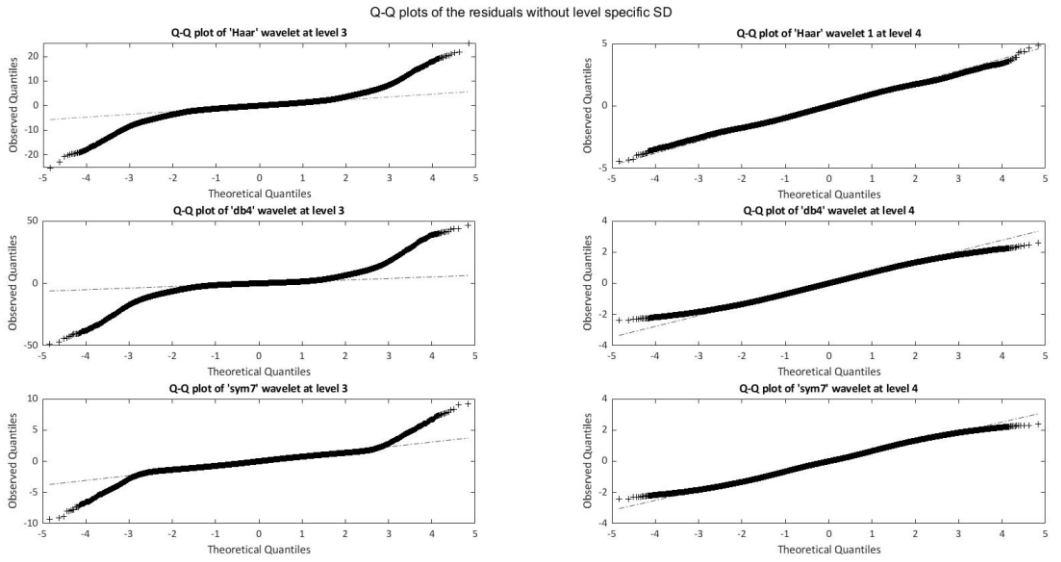

Figure 8: Q-Q plots of residuals at different levels of decomposition and with different wavelets, with a threshold with non-level-dependent SD. Time interval 0 – 80s.

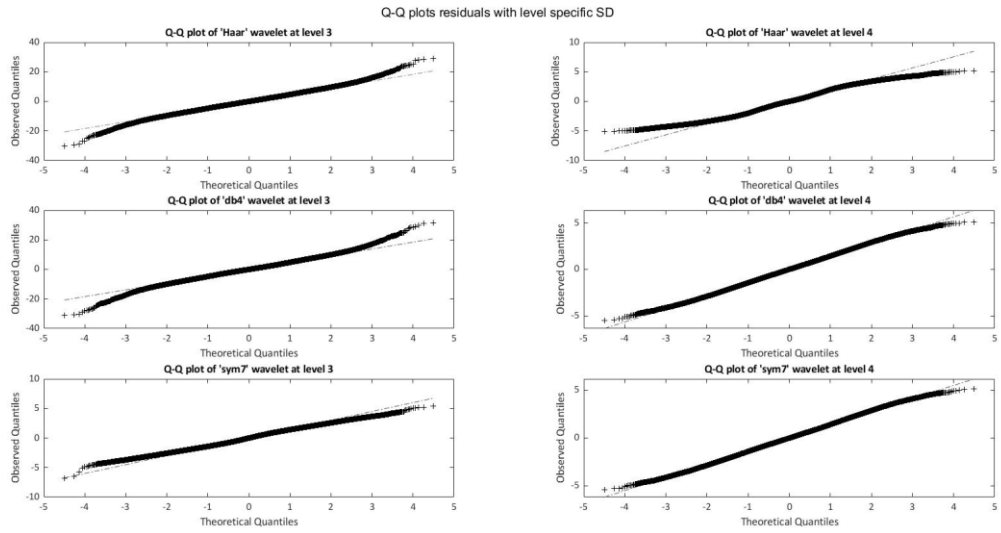

Figure 9: Q-Q plots of residuals at different levels of decomposition and with different wavelets, with a threshold with level-dependent SD. Time interval 60 – 75s, during Valsalva.

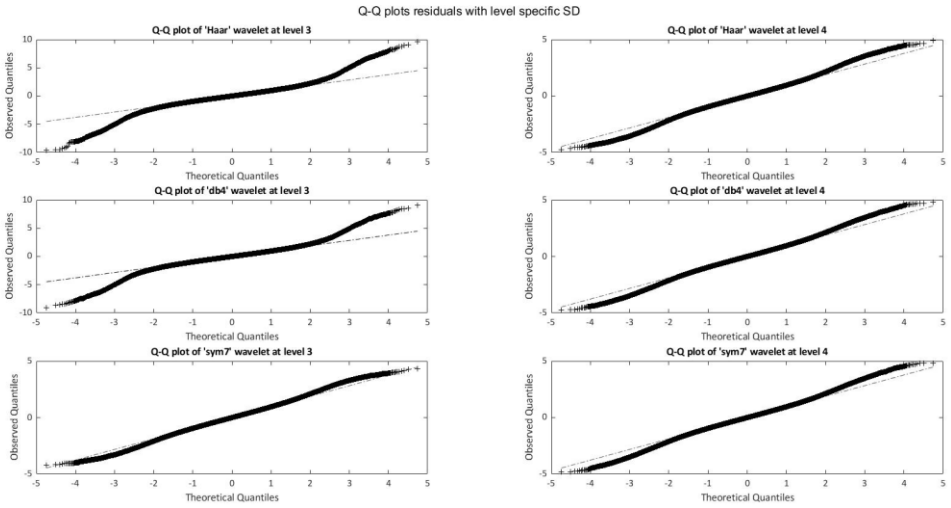

Figure 10: Q-Q plots of residuals at different levels of decomposition and with different wavelets, with a threshold with level-dependent SD. Time interval 1 – 50s, in rest.

Appendix C: Statistics

Normal distribution tests

Data from a small sample is often not normally distributed. To prevent making a type 1 error during statistical analysis, it is necessary to test if our data is normally distributed before performing any statistical test. Fisher's measure of skewness and kurtosis is a widely used method to analyse the shape of the distribution of a data set. Skewness and kurtosis are measures of asymmetry and *peakedness* of a distribution, respectively [69]. The skewness can be calculated with the use of equation 8 and the kurtosis with equation 9 [70].

$$\gamma_1 = \frac{\sqrt{n(n-1)}}{n-2}\frac{m_3}{m_2^{3/2}} \tag{8}$$

$$\gamma_2 = \frac{n-1}{(n-2)(n-3)}\left\{(n+1)\left(\frac{4}{m_2^2}-3\right)+6\right\} \tag{9}$$

With $m_k = \sum_{i=1}^{n}(x_i - \bar{x})^k/n$ and n the amount of samples

Values of $\gamma_1$that are positive mean that the curve of the distribution of the data is right-skewed or right-tailed and negative values indicate left skewing. A value of γ_1 that approaches zero indicates symmetry. Positive values of γ_2 indicate a more peaked distribution and negative values indicate a distribution that is flatter than the normal distribution. A value of γ_2 that approaches zero indicates an identical kurtosis to a normal distribution [69]. A non-normal distribution must be regarded when γ_1 < -1 or γ_1 > 1 and the same applies to γ_2. At last, a Z-test can be used to test for normality. To do this, you first must calculate the standard error of the skewness and kurtosis and divide the skewness and kurtosis by this standard error. If absolute Z-scores are larger than 1.96, corresponding with a significance level of 0.05, conclude that the distribution of the sample is non-normal [71].

After analysis of skewness and kurtosis, the data was classified as not normally distributed. We transformed the data in different ways, after which analysis of skewness and kurtosis was again performed. However, even after transformation the data was still not normally distributed.

Wilcoxon signed-rank test

We decided to analyse difference in SNR between leads with the Wilcoxon signed-rank test, because data then does not need to be normally distributed.

The Wilcoxon signed-rank test is an alternative for the dependent T-test when the data is not normally distributed. The test calculates the differences between measurements on the same person, after which these differences are analysed to determine if the differences are statistically significant. When the two tailed exact significance level is smaller than 0.05 the measurement outcomes are significantly different with $\alpha = 5\%$. The Wilcoxon signed-rank test can be defined by equation 10, 11 and 12 [38]:

$$T_c^{(obs)} = \sum_{i=1}^{m} S_{i+} = \sum_{i=1}^{m}\sum_{j=1}^{g} R_{ij}V_{ij} \tag{10}$$

$$T_c = \sum_{i=1}^{m} \delta_i S_{i+} \tag{11}$$

$$p = 2 \times \min\{\Pr(T_c \geq T_c^{(obs)}), \Pr(T_c \leq T_c^{(obs)}), 0.5\} \tag{12}$$

In the analysis of our data, this test was used to determine differences between SNR in lead positions. The leads with the best SNR were selected to use for analysis of influences of patient characteristics on the SKNA signal.

Mann-Whitney test

The Mann-Whitney test is a commonly used alternative for the independent T-test when the data is not normally distributed. This test is similar to the Wilcoxon Rank-Sum test. The test determines the probability that two different groups are statistically the same. The groups do not have the same distribution and thus are significantly different for a two-tailed exact significance level of < 0.05 [72].

The assumptions of the test are:

- The two investigated groups are randomly drawn from the target population.
- Each measurement is from a different participant.
- The dependent variable is ordinal or continuous and the independent values are ordinal, relative, or absolute.

The Mann-Witney test can be mathematically defined by equation 13, 14 and 15 [73]:

$$U_x = n_x n_y + \frac{n_x(n_x+1)}{2} - R_x \quad (13)$$

$$U_y = n_x n_y + \frac{n_y(n_y+1)}{2} - R_y \quad (14)$$

$$\sigma_U = \sqrt{((n_x n_y)(N+1))/12} \quad (15)$$

With test statistic: $|z| = \frac{|U_x+U_y|}{\sigma U}$

n_x is the total number of observations in the first group. n_y is the total number of observations in the second group. R_x and R_y are respectively the sum of the ranks assigned to group x and group y. The test statistic is the absolute value of z, and the z-table is used to determine the critical value corresponding to the chosen significance level. There is a significant result if z is equal to or bigger than the z-table value of the chosen significance level [73]. In the analysis of our data, this test was used to determine possible influence of sex and BMI on the SKNA signal. The data was split in groups based on BMI or sex, after which the Mann-Whitney test determined whether differences in signal exists between groups.

Kruskal-Wallis one-way analysis of variance

The Kruskal-Wallis test is a non-parametric test that compares an outcome measure between groups and determines whether at least one of these groups statistically significantly differs from the other groups. It does not determine which of the groups is different from the others. The test ranks the data of all groups from low to high, with ties being represented by the average of the ranks that would be assigned if there were no ties. Based on the total and average rank scores per group, the H statistic is calculated. The Kruskal-Wallis test assumes that all measurements are independent, that all measurements in a sample originate from the same population and that all measurements follow the same distribution. The Kruskal-Wallis test can be represented mathematically with equations 16 and 17 [39].

$$H = \frac{12}{N(N+1)} \sum_{i=1}^{C} \frac{R_i^2}{n_i} - 3(N+1) \quad (16)$$

$$H = \frac{H}{1-\frac{\sum T}{N^3-N}} \quad (17)$$

C is the number of samples in the study, in other words the number of different groups in the analysis. The value N is the sum of all observations in all the samples combined. R_i is the sum of ranks of each independent sample. n_i is the number of observations in each sample. In the H statistic the means of the different samples are compared to test the overall closeness to each other. Depending on the conditions of the study, the H statistic will be compared to different statistic tables. If C is more than 3 and the n_i in each sample is more than 5, the Chi-square table values of $df = C - 1$ can be used to determine the tabled value. The null hypothesis is rejected if the H-statistic is larger than the tabled. In case of more than 3 samples, but an n_i less than 5, the Kruskal Wallis critical values table is used. In this case, the H-statistic is smaller than the tabled value, the null hypothesis is rejected. In case of ties in the ranks, a correction factor must be applied on the H statistic from the first equation. A sum of T-correction factor is used, to calculate the adjusted H statistic: $T = t_i^3 - t_i$, where t_i is the number of tied ranks in the i_{th}sample. We did not expect any ties in our data [39].

To determine which of the groups is significantly different from the others, multiple comparisons among treatments can be used. This method can be represented mathematically with equation 18 [39].

$$|\overline{R_u} - \overline{R_v}| \geq \frac{Z_\alpha}{i(i-1)} \sqrt{\frac{N(N+1)}{12}\left(\frac{1}{n_u} + \frac{1}{n_v}\right)} \tag{18}$$

Here different groups are noted by u and v. To reject the null hypothesis, the absolute difference between the means is calculated and compared to the critical difference. The critical difference is calculated by taking the Z_α of the chosen significance level and adapting it according to equation 18. If the absolute difference between the means of the samples is greater than the critical difference, the null hypothesis is rejected and the difference between the samples is statistically significant [39].

Friedman test

The Friedman test is a non-parametric statistical test for repeated measurements that determines whether one of the groups that are being compared consistently outscores the other groups. The test accomplishes this by assigning ranks to the measurement in a certain group. In every group, the different measurements are ranked from low to high. If two measurements are tied, the assigned rank will be the average of the ranks that would be assigned if there were no ties. The Friedman test can be represented mathematically with equation 19 [37].

$$\chi_r^2 = \frac{12}{Nk(k+1)} \sum_{j=1}^{k} R_j^2 - 3N(k+1) \tag{19}$$

k is the number of ranked observations, also called a sample. N is the number of subjects and R_j is the sum of the rank of the k_{th} sample. The test statistic χ_r^2 is compared to the χ^2 distribution to test the statistical significance of the result. The number of degrees of freedom for the χ^2 distribution for the test is $k - 1$ [37].

Comparably to the Kruskal-Wallis test, the Friedman test only determines whether one or more of the groups differs significantly from the other groups, while it does not determine which of the groups is significantly different from the others. As with the Kruskal-Wallis test, a pairwise comparison of groups can be used to determine which differences are statistically significant. Wilcoxon signed-rank tests can be used for this comparison.

Appendix D: Information letter

Proefpersonen Informatieformulier

Huidzenuwmetingen aan individuen zonder hartziekten van verschillend geslacht en BMI om de zenuwactiviteit van de ganglion stellatum in rust te bepalen.

Geachte meneer/mevrouw,

U bent recent benaderd door een van de onderzoekers om mee te doen aan het door hen benoemde onderzoek. We vragen u vriendelijk om deel te nemen aan dit onderzoek. Via dit formulier kunt u een weloverwogen keuze maken of u dit wilt.

Om deze keuze te kunnen maken is het belangrijk u goed in te lezen in de informatie die in dit formulier verstrekt wordt. Overleg uw deelname met uw partner, vrienden of familie voor u de keuze maakt. Mocht u na het lezen van dit formulier nog vragen hebben dan kunt u contact opnemen met een van de onderzoekers. De contactgegevens staan onderaan dit formulier.

Wat is het doel van het onderzoek?

Onderzoekers aan de Universiteit Twente en het MST werken aan een nieuwe meettechniek om de zenuwactiviteit van de ganglion stellatum te bepalen. Dit is een zenuwknoop die ligt in de nek en die elektrische signalen stuurt naar ons hart. Sommige patiënten met hartritmestoornissen ervaren, ondanks hun medicatie en/of defibrillator, terugkerende aanvallen van een verstoord hartritme. De oorzaak kan dan in deze zenuwknoop liggen. Om te onderzoeken of het nut heeft om deze knoop chirurgisch te verwijderen, wordt er lokaal een zenuwverlammend medicijn in de knoop geïnjecteerd. Als de ritmestoornissen verdwijnen, is het zinvol om de knoop chirurgisch door te snijden. Gebeurt dit niet, dan is het niet zeker of de knoop daadwerkelijk verlamd is of dat de ritmestoornissen een andere oorzaak hebben. Dit komt doordat er nog geen effectieve techniek is om de activiteit van de zenuwknoop te meten. De onderzoekers aan de Universiteit Twente en het MST onderzoeken nu een manier om te kijken of het mogelijk is door middel van een nieuwe techniek de activiteit van de zenuwknoop te meten. Hierbij is het belangrijk om te weten wat deze activiteit is in gezonde proefpersonen en hoe deze afhangt van de locatie van de elektroden, geslacht en BMI. Daarvoor wordt dit onderzoek gedaan. In dit onderzoek zullen dan ook geen zenuwverlammende medicijnen gebruikt worden.

Hoe wordt het onderzoek uitgevoerd?

Voor dit onderzoek vragen wij u om naar het MST in Enschede te komen, het adres en de afdeling in het ziekenhuis staan onderaan dit formulier. De datum en tijdstip van het bezoek wordt in overleg met u afgesproken. Bij binnenkomst vragen wij u of u nog vragen heeft en of u een formulier wilt ondertekenen dat de onderzoekers toestemming geeft om uw resultaten te gebruiken.

Bij de start van het onderzoek en noteren wij eerst uw leeftijd, geslacht, lengte en gewicht. Daarna zal een van de onderzoekers zes elektroden plakken op uw linkerarm en zes op de borstkast. Dit zijn dezelfde elektroden die worden gebruikt voor het maken van een hartfilmpje (ECG). Het apparaat (Biomonitor ME6000) meet de elektrische activiteit van de hartspier en activiteit van de zenuwen in de huid. U moet hiervoor uw bovenkleding, behalve uw BH/ hemd, uittrekken.

Tijdens het onderzoek zal aan u gevraagd worden om na een periode van rust een Valsalva manoeuvre uit te voeren. Dit is een simpele manier om de het zenuwstelsel te activeren. Bij de Valsalva manoeuvre moet u ongeveer 15 seconden met uw neus en mond dicht op uw hand blazen. Hierdoor wordt er een lichte druk in het lichaam opgebouwd, waardoor het zenuwstelsel geactiveerd wordt. Het is eigenlijk een beetje vergelijkbaar met het opblazen van een ballon. Dit is een veilige manoeuvre en brengt geen nadelige effecten met zich mee.

Tijdens de meting zal een van de onderzoekers controleren of de metingen correct zijn vastgelegd. Als dit zo is worden de elektroden weer verwijderd en is het onderzoek afgelopen. Het gehele onderzoek zal maximaal drie kwartier duren.

Wat wordt er van u verwacht?

U wordt gevraagd om toestemming te geven om bovenstaande metingen te mogen uitvoeren. Daarnaast wordt u gevraagd toestemming te geven om de verderop aanvullende medische gegevens te mogen verzamelen en verwerken door het onderzoeksteam.

Het is belangrijk dat u eerlijke informatie verstrekt voorafgaand aan het onderzoek over het volgende:

- Als u een hartpatiënt bent kunt u niet meedoen aan het onderzoek, ook als u bloeddrukverlagende medicatie gebruikt.
- Als u een aandoening hebt aan uw zenuwstelsel kunt u niet meedoen aan het onderzoek.
- Drink geen koffie voorafgaand aan uw onderzoek. U mag uw laatste kop koffie 12 uur van tevoren nemen. Ditzelfde geldt voor alle cafeïnerijke voedingsmiddelen.
- U mag niet onder de invloed van stimulerende middelen zoals alcohol of drugs zijn tijdens het onderzoek.

Daarnaast verwachten wij u op tijd op de locatie zodat er nog ruimte is voor vragen en het invullen van het toestemmingsformulier.

Onverwachte bevindingen

De metingen die worden uitgevoerd geven informatie over het functioneren van uw hart en/of zenuwstelsel. Hierdoor is het mogelijk dat er onverwachts afwijkingen gevonden worden, zoals een afwijkend hartritme. In een dergelijk geval zal u op de hoogte gesteld worden door de onderzoeker. U moet realiseren dat de verkregen data niet wordt beoordeeld vanuit een medisch perspectief, deelname kan daarom ook niet aangezien worden voor een medische test.

Wat gebeurt er als u niet wenst deel te nemen aan dit onderzoek?

U beslist zelf of u meedoet aan het onderzoek. Deelname is vrijwillig. Als u besluit niet mee te doen, hoeft u verder niets te doen. Als u wel meedoet, kunt u zich altijd bedenken en toch stoppen. Ook tijdens het onderzoek. U hoeft geen reden te geven waarom u wilt stoppen.

Wat gebeurt er met uw gegevens?

Om te voldoen aan de privacywetgeving van de AVG worden uw gegevens geanonimiseerd waardoor ze niet te koppelen zijn aan u als persoon. Alleen de onderzoekers kunnen bij de data en deze worden niet vrijgegeven. Uw geanonimiseerde gegevens worden voor een periode voor 15 jaar op een beschermde server van het MST bewaard.

Deze gegevens betreffen: geslacht, leeftijd, lengte, gewicht en resultaten van de metingen. Het verzamelen, gebruiken en bewaren van uw gegevens is nodig om de vragen die in dit onderzoek worden gesteld te kunnen beantwoorden en de resultaten te kunnen publiceren. Wij vragen voor het gebruik van uw gegevens uw toestemming.

Intrekken toestemming

U kunt uw toestemming voor gebruik van uw persoonsgegevens altijd weer intrekken. De onderzoeksgegevens die zijn verzameld tot het moment dat u uw toestemming intrekt worden nog wel gebruikt in het onderzoek. Tot slot kunnen alle onderzoekers ten alle tijden besluiten om het onderzoek te beëindigen als u niet geschikt bent voor deelname.

Zijn er extra kosten of krijgt u een vergoeding wanneer u besluit aan dit onderzoek mee te doen?
U maakt geen kosten voor het onderzoek. U krijgt geen vergoeding voor deelname aan het onderzoek.

Door wie is dit onderzoek goedgekeurd?
De ethische commissie van de faculteiten Technische Natuurwetenschappen (TNW) en Engineering Technology (ET) van de Universiteit Twente heeft goedkeuring gegeven om dit onderzoek uit te voeren.

Heeft u klachten over dit onderzoek?
Bij klachten over het onderzoek kunt u contact opnemen met het secretariaat van de ethische commissie van de faculteiten Technische Natuurwetenschappen (TNW) en Engineering Technology (ET),
P.O. Box 217, 7500 AE Enschede (NL),
telefoon: +31 (0)534895607
email: a.m.klijnstra@utwente.nl

Wilt u meer informatie?
Voorafgaand aan de metingen is er ruimte om vragen te beantwoorden. Mocht u op dit moment vragen hebben dat kunt u contact opnemen met een van de onderzoekers waarvan de gegevens vermeld zijn onderaan dit formulier.

Heeft u besloten om deel te nemen aan het onderzoek?
Neem dan contact op met een van de onderzoekers waarvan de gegevens vermeld zijn onderaan dit formulier om een afspraak te maken voor het onderzoek.

Bij voorbaat hartelijk dank.

Met vriendelijke groet,

Contact:
T. Voortman
E-mail: t.voortman@student.utwente.nl
T: +31 637375753

N.J. Bergwerff
E-mail: n.j.bergwerff@student.utwente.nl
T: +31 640897409

L.M. Dolmans
E-mail: l.m.dolmans@student.utwente.nl
T: +31 683540614

N. van Dieren
E-mail: b.j.vandieren@student.utwente.nl
T: +31 613163702

Locatie:
MST, koningsplein 1, Enschede.
Afdeling: Cardiologie, Route: A25

Toestemmingsformulier

Titel: “Huidzenuwmetingen aan individuen zonder hartziekten van verschillend geslacht en BMI om de zenuwactiviteit van de ganglion stellatum in rust te bepalen.”

- Ik heb de informatiebrief voor deelname aan het onderzoek gelezen. Ik kon aanvullende vragen stellen. Mijn vragen zijn genoeg beantwoord. Ik had genoeg tijd om te beslissen of ik meedoe.
- Ik weet dat meedoen helemaal vrijwillig is. Ik weet dat ik op ieder moment kan beslissen om toch niet mee te doen. Daarvoor hoef ik geen reden te geven.
- Ik weet dat sommige mensen mijn gegevens kunnen zien. Die mensen staan vermeld in de informatiebrief.
- Ik geef toestemming om mijn gegevens te gebruiken, voor de doelen die in de informatiebrief staan.
- Ik wil meedoen aan dit onderzoek.

Naam deelnemer:
Handtekening: Datum : __ / __ / __

Ik verklaar hierbij dat ik deze deelnemer volledig heb geïnformeerd over het genoemde onderzoek.
Als er tijdens het onderzoek informatie bekend wordt die de toestemming van de deelnemer zou kunnen beïnvloeden, dan breng ik hem/haar daarvan tijdig op de hoogte.

Naam onderzoeker (of diens vertegenwoordiger):
Handtekening: Datum: __ / __ / __

Aanvullende informatie is gegeven door (indien van toepassing):
Naam:
Functie:
Handtekening: Datum: __ / __ / __
---
* Doorhalen wat niet van toepassing is.

Appendix E: Excluded measurements

Based on the SQI, 42 measurements were excluded for various reasons. These reasons being:

- The signal does not exist for three minutes
- There are regular noise pulses in the aSKNA signal
- The raw signal does not look random
- Valsalva manoeuvre does not lead to an increase in the signal

Examples of excluded measurements can be found in figure 11,12,13 and 14.

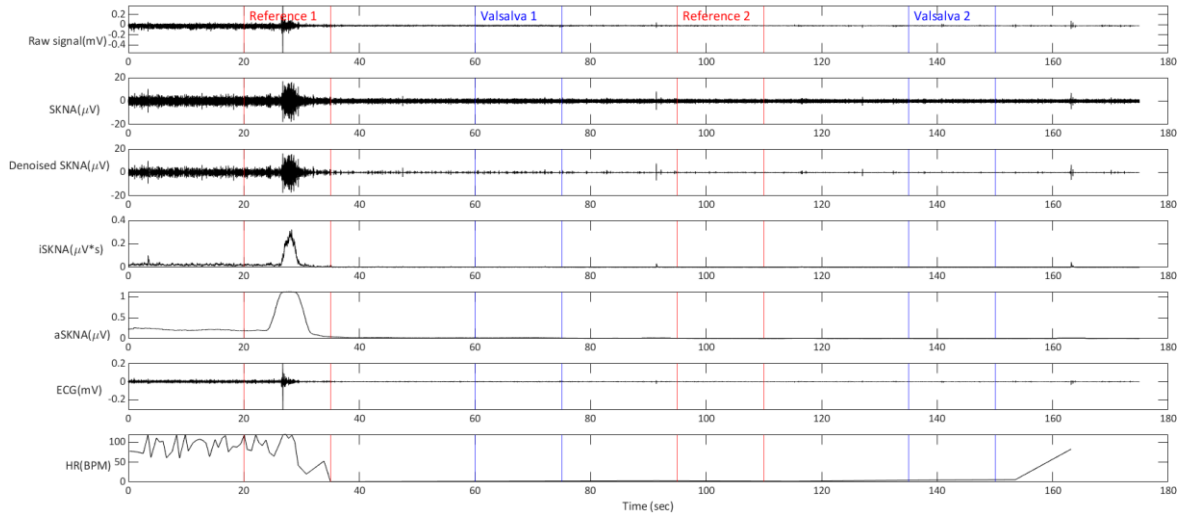

Figure 11: Example of a measurement excluded because it did not have signal during the entire measurement

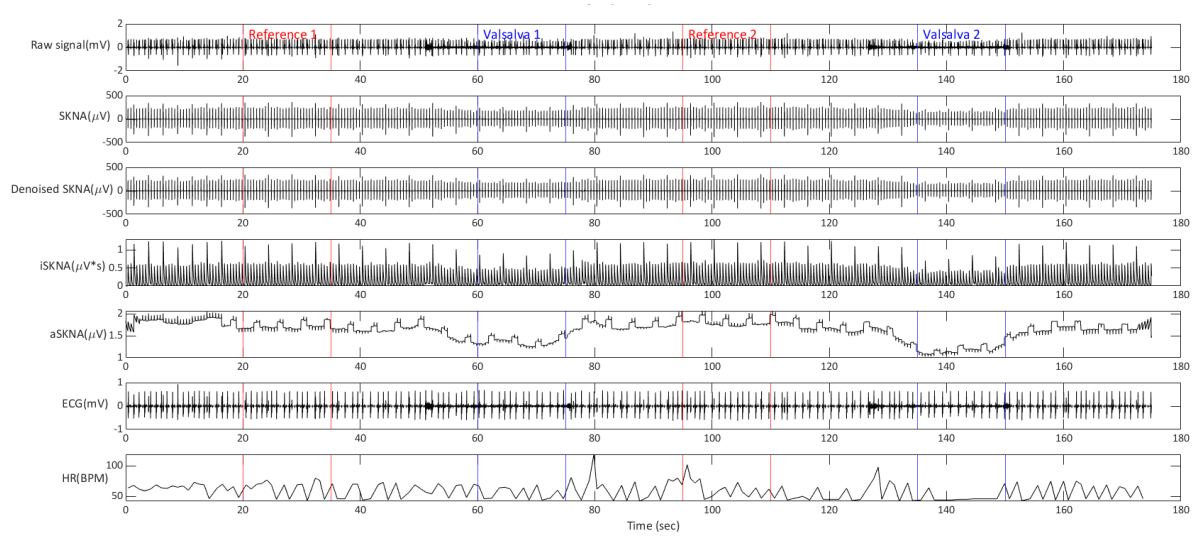

Figure 12: Example of a measurement excluded because of repeating noise pulses in the aSKNA signal

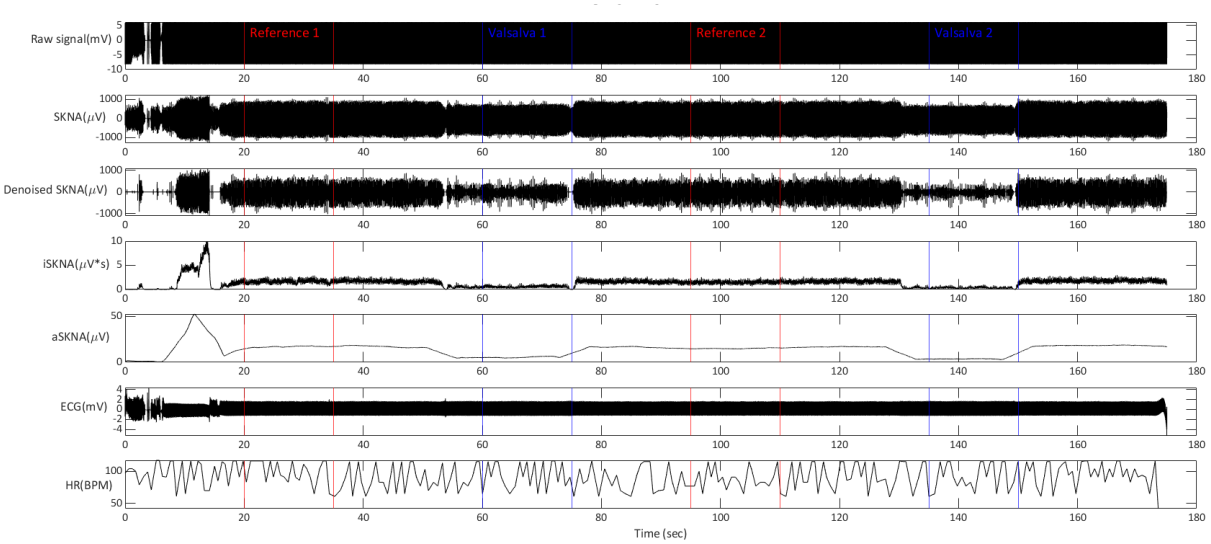

Figure 13: Example of a measurement excluded because a lack of randomness in the raw signal

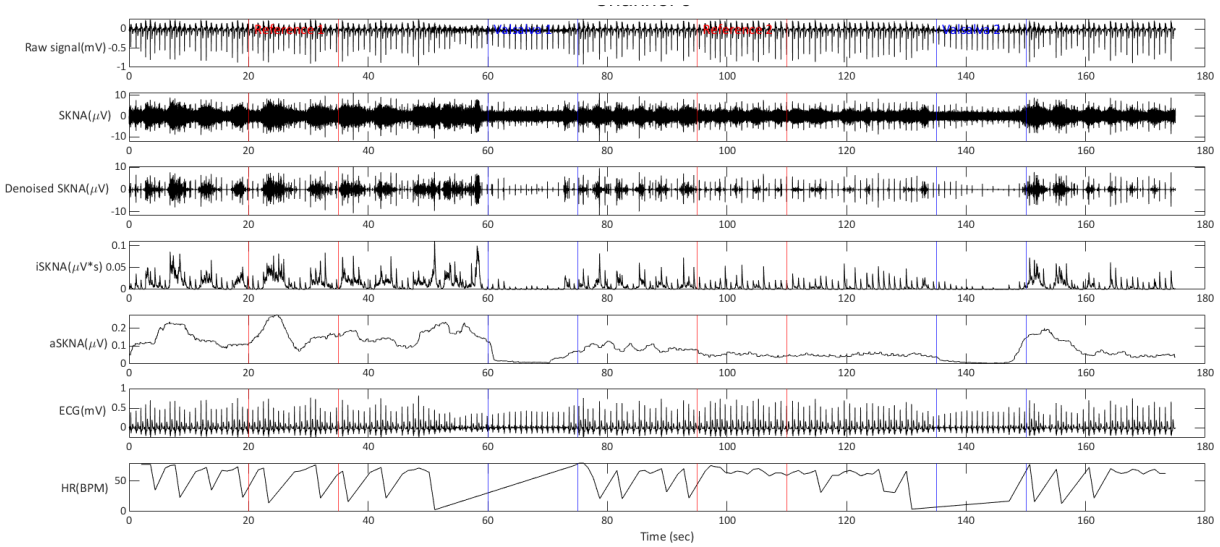

Figure 14: Example of measurement excluded because of a lack of increase in the aSKNA signal during Valsalva manoeuvre

Appendix F: Table of used acronyms and abbreviations

Acronym/abbreviation	Definition
ΔaSKNA	Difference in average skin sympathetic nerve activity between rest and Valsalva
aSKNA	Average skin sympathetic nerve activity
$aSKNA_{rest}$	Average skin sympathetic nerve activity in rest
$aSKNA_{vals}$	Average skin sympathetic nerve activity during Valsalva
BMI	Body Mass Index
CMs	Cardiomyocytes
CWT	Continuous wavelet transform
Db4	Daubechies 4
DWT	Discrete wavelet transform
ECG	Electrocardiography
HR	Heart rate
iSKNA	Integrated skin sympathetic nerve activity
MI	Myocardial infarction
NA	Noradrenaline
PNs	Parasympathetic nerves
SCNA	Subcutaneous nerve activity
SD	Standard deviation
SGNA	Stellate ganglion nerve activity
SKNA	Skin sympathetic nerve activity
SNR	Signal to noise ratio
SNs	Sympathetic nerves
SQI	Signal Quality Index
SWT	Stationary wavelet transform
Sym7	Symlets 7